Supporting Information

Discovery of McrA, a master regulator of *Aspergillus* secondary metabolism

C. Elizabeth Oakley[1], Manmeet Ahuja[1,2], Wei-Wen Sun[3], Ruth Entwistle[1], Tomohiro Akashi[4], Junko Yaegashi[3,5], Chun-Jun Guo[3,6], Gustavo C. Cerqueira[7], Jennifer Russo Wortman[7], Clay C. C. Wang[3,9], Yi-Ming Chiang[3,9] and Berl R. Oakley[1]*

[1] Department of Molecular Biosciences

University of Kansas

1200 Sunnyside Avenue

Lawrence, Kansas 66045

USA

[2]Current address: Industrial Biotechnology Division

Reliance Technology Group, Reliance Industries Limited

Reliance Corporate Park

Thane Belapur Road, Ghansoli, Navi Mumbai 400701

India

[3] Department of Pharmacology and Pharmaceutical Sciences

School of Pharmacy

University of Southern California

1985 Zonal Avenue,

Los Angeles, California 90089

USA

[4]Division of OMICS analysis

Nagoya University Graduate School of Medicine

65 Tsurumai, Nagoya, Aichi 466-8550

Japan

[5]Current addresses: Joint BioEnergy Institute

5885 Hollis St., Emberyville, CA 94608

and Pacific Northwest National Laboratory

902 Battelle Blvd., Richland, WA 99354

[6]Current address: Department of Bioengineering and Therapeutic Sciences

University of California, San Francisco

1700 4th St., San Francisco, CA 94143

[7]Genome Sequencing and Analysis Program

Broad Institute of MIT and Harvard

415 Main St.

Cambridge, MA 02142

USA

[8] Department of Chemistry

Dornsife Colleges of Letters, Arts, and Sciences

University of Southern California

Los Angeles, California 90089

USA

[9] Department of Pharmacy

Chia Nan University of Pharmacy and Science

Tainan City 71710

Taiwan

Republic of China

*Corresponding author: boakley@ku.edu

Table of Contents

Detailed Structural Characterization of Compounds 12 and 13

Compound **12** was isolated as a pale yellow powder. The molecular formula was found to be $C_{15}H_{19}NO_5$ from HRESIMS and ^{13}C NMR data. Cichorine (**10**)(*Sanchez et al*., 2012) and compound **12** were isolated from the same fraction and they have similar UV-Vis absorption spectra (Fig. S11), suggesting that **12** contains a cichorine-like chromophore. Comparing ^{1}H and ^{13}C NMR data of **12** with those of **10** supported the cichorine partial structure of **12** (Table S5). Besides the cichorine moiety, the ^{1}H and ^{13}C NMR data also exhibited a carboxybutyl spin system [δ_H 1.62 and 1.73 (each 2H, m), 2.36 and 3.61 (each 2H, t); δ_C 23.3 (CH_2), 28.9 (CH_2), 34.4 (CH_2), 43.2 (CH_2), 177.4 (C)], suggesting compound **12** is carboxybutyl cichorine. HMBC correlations between C-1/H_2-11 and C-8/H_2-11 established that **12** is *N*-(4-carboxybutyl)cichorine. COSY, HMQC, and HMBC NMR spectral data all support the assigned structure of **12**.

Compound **13** has twenty carbon signals in its ^{13}C NMR spectrum. In its ESI mass spectrum (Fig. S11), however, it shows no obvious parent ion with twenty carbons detected and the base peak was at *m*/*z* 181 (positive mode), suggesting that **13** might be unstable during the ionization process. In its ^{1}H and ^{13}C NMR spectra (Table S5), **13** exhibited 4 methyl groups attached to benzene rings [δ_H 2.06, 2.09, 2.31, and 2.46 (each 3H, s); δ_C 8.6, 9.1, 20.1, and 21.9], two methoxy groups [δ_H 3.66 and 3.79 (each 3H, s); δ_C 62.2 and 63.6], two aromatic protons [δ_H 6.38 and 6.46 (each 1H, s)], and one benzaldehyde group [δ_H 10.26 (1H, s); δ_C 192.8]. In its ^{13}C NMR spectrum, there are a total of 12 carbons in the aromatic region (from 110 to 170 ppm), suggesting that compound **13** contains two benzene rings. Since there are only two singlet aromatic protons, compound **13** was proposed to contain two penta-substituted benzene rings. Several signals, such as methyl, methoxy, and aromatic groups, appeared to be paired in its ^{1}H and ^{13}C NMR spectra (Table S5), indicating that **13** might be a dimer of two similar penta-substituted benzenes. The ^{1}H and ^{13}C NMR spectra from a single set of penta-substituted benzene ring of **13**, moreover, exhibit a similar pattern of chemical shift as 3-methylorsellinic acid, an NRPKS product isolated from an AN6448 overexpressing strain (Ahuja *et al.*, 2012). This suggests **13** is a dimer of two 3-methylorsellinic acid derivatives. HMQC and long-range HMBC correlations allowed full assignment of the structure (Fig. S12 and Table S5). Compound **13** is a dimer of the *O*-methyl-3-methylorsellinaldehyde with a hemiacetal linkage. Hemiacetal is not stable and, therefore, it fragments during the electrospray ionization process (Fig. S11).

Isolation of Secondary Metabolites

For scaling up to isolate compounds **12** and **13**, 50 15-cm GMM plates (3 L of medium in total) inoculated with *A*. *nidulans* strain LO8111 were grown for 5 days at 37°C. The agar was chopped into pieces and extracted with 2.5 L of MeOH and then 2.5 L of 1:1 dichromethane-methanol as described in Materials and Methods. After removing the solvent *in vacuo*, the total crude extract (~5.0 g) was applied to a reverse phase C18 gel column (COSMOSIL 75C18-OPN, 35 × 150 mm) and eluted with MeOH-H_2O mixtures of decreasing polarity (fraction A, 1:9, 250 ml; fraction B, 3:7, 250 ml; fraction C, 7:3, 250 ml; fraction D, 1:0, 100 ml). Fraction B (~270 mg) containing compounds **12** and **13** was subjected to purification by semi-preparative reverse phase HPLC [Phenomenex Luna 5 μm C18 (2), 250 × 10 mm] and monitored by a PDA detector at 236 nm. The gradient system (5 ml/min) was MeCN (solvent B) in 5% MeCN/H_2O (solvent A) with the following gradient conditions: 5 to 40% B from 0 to 20 min, 40 to 100% B from 20 to 21 min, maintained at 100% B from 21 to 22 min, 100 to 5% B from 22 to 23 min, and re-equilibration with 5% B from 23 to 27 min. Compounds **12** (2.9 mg) and **13** (4.8 mg) were eluted at 16.7 and 20.6 min, respectively. Cichorine (**10**, 6.7 mg) eluted at 12.8 min was also isolated from this fraction. In addition, 3.0 mg of felinone A (**14**) eluted at 7.5 min was also isolated.

Compound Spectral Data

NMR spectral data were collected on a Varian Mercury Plus 400 spectrometer. High resolution electrospray ionization mass spectrum was obtained on an Agilent 6210 time of flight LC-MS. Optical rotations were measured on a JASCO P-2000 digital polarimeter.

N-(4-Carboxybutyl)cichorine (**12**)

Pale yellow powder; For UV-Vis and ESIMS spectra, see Fig. S5; For ^{1}H and ^{13}C NMR data (CD_3OD), see Table S4; HRESIMS, $[M - H]^-$ *m/z* found 292.1189, calc. for $C_{15}H_{20}NO_5$: 292.1185.

O-Methyl-3-methylorsellinaldehyde dimer (**13**)

Pale yellow oil; $[\alpha]_D^{25}$ 2.4° (MeOH *c* 0.3); For UV-Vis and ESIMS spectra, see Fig. S5; For ^{1}H and ^{13}C NMR (CD_3OD), see Table S4.

Felinone A (**14**)

Pale yellow oil; $[\alpha]_D^{25}$ 101.4° (MeOH *c* 0.2); For UV-Vis and ESIMS spectra, see Fig. S5; ^{1}H and ^{13}C NMR data (CD_3OD), in good agreement with the published data (Du *et al.*, 2014) .

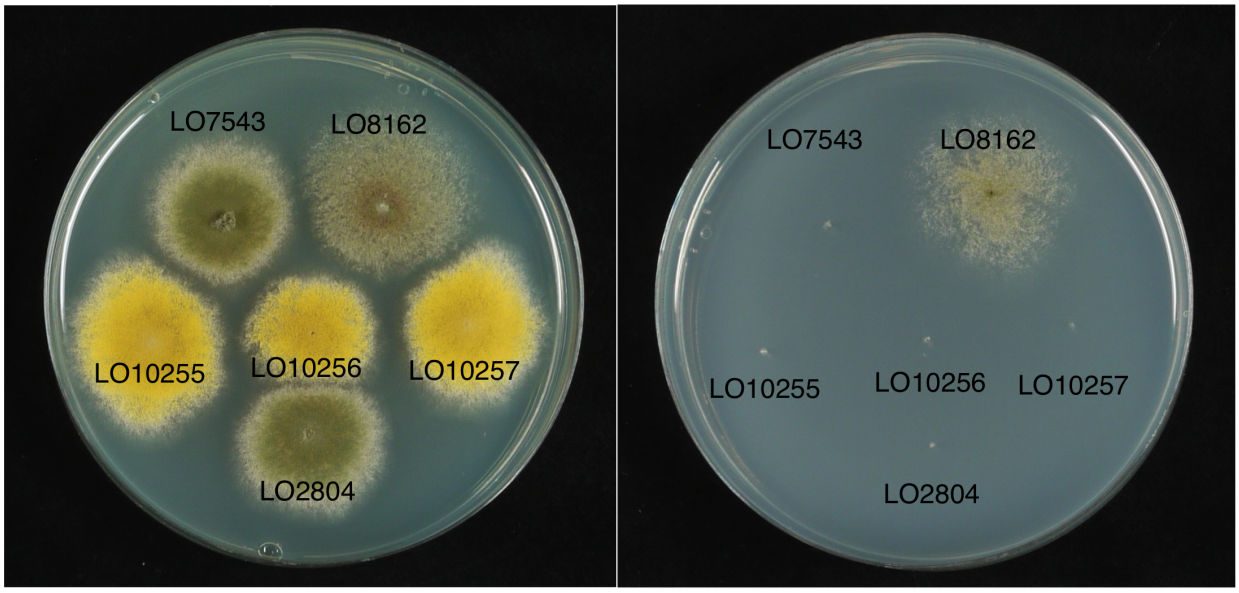

Figure S1. Reinsertion of AN8694 (*mcrA*) at the at the *yA* locus restores riboflavin auxotrophy. The plate at the left contains minimal medium supplemented for riboflavin and it allows the growth of strains that require riboflavin. The plate at the right is identical except that riboflavin is omitted and only riboflavin prototrophs grow. (Both plates are supplemented with pyridoxine which is required by all of these strains.) LO7543 carries a replacement of the AN1242 coding sequence with the *Aspergillus fumigatus riboB* coding sequence. Since the AN1242 promoter is inactive no growth occurs in the absence of the riboflavin supplement. LO8162 carries a deletion of AN8694 (*mcrA*) which activates expression of the AN1242 promoter, allowing growth without riboflavin. In LO10255, LO10256, and LO10257, a copy of AN8694 has been reinserted at the *yA* locus of LO8162, causing the colonies in these transformants to be yellow. Reinsertion of AN8694 also restores riboflavin auxotrophy, thus confirming that the AN8694 deletion was responsible for activation of the AN1242 promoter and consequent riboflavin prototrophy. Reinsertion of AN8694 also restores more robust growth. LO2804 is a riboflavin auxotrophic control strain. It is LO1362 transformed with a wild-type copy of the *A. nidulans pyrG* gene to complement the pyrimidine requirement of LO1362 and allow growth on media unsupplemented for uridine and uracil, but it carries *riboB*2 and requires riboflavin for growth.

A.

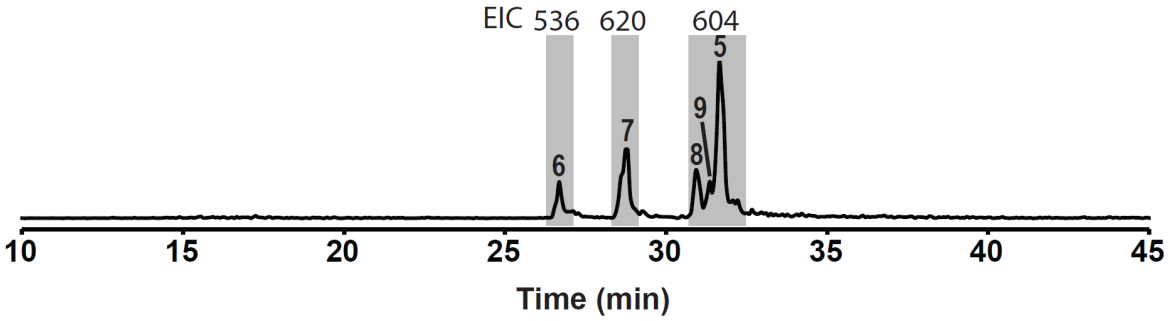
EIC 536 620 604
6
7
8
9
5
10
15
20
25
30
35
40
45
Time (min)

B.

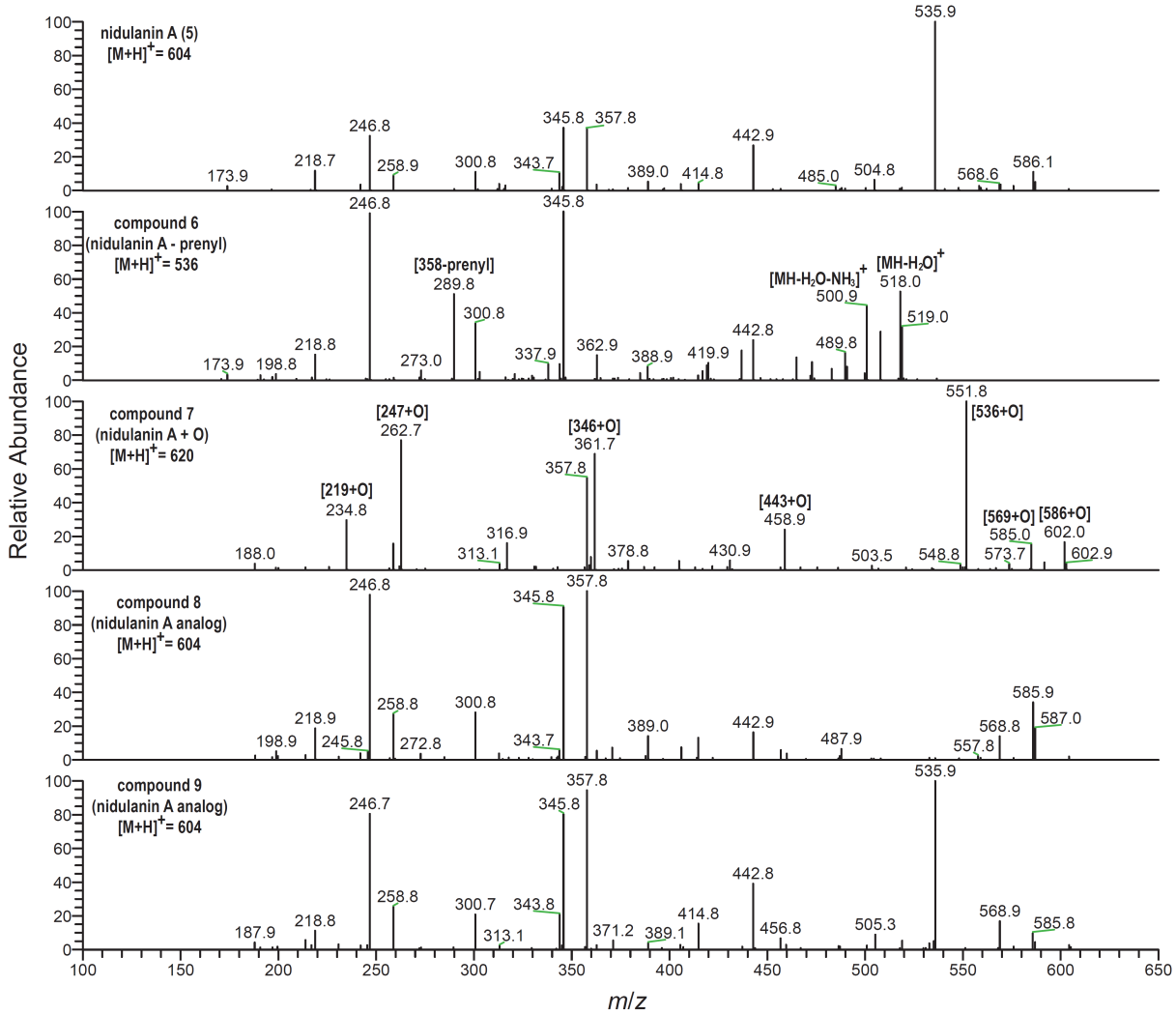
nidulanin A (5)
[M+H]+= 604
compound 6
(nidulanin A - prenyl)
[M+H]+= 536
[358-prenyl]
[MH-H2O-NH3]+
[MH-H2O]+
compound 7
(nidulanin A + O)
[M+H]+= 620
[247+O]
[346+O]
[219+O]
[443+O]
[536+O]
[569+O]
[586+O]
compound 8
(nidulanin A analog)
[M+H]+= 604
compound 9
(nidulanin A analog)
[M+H]+= 604
Relative Abundance
m/z

C.

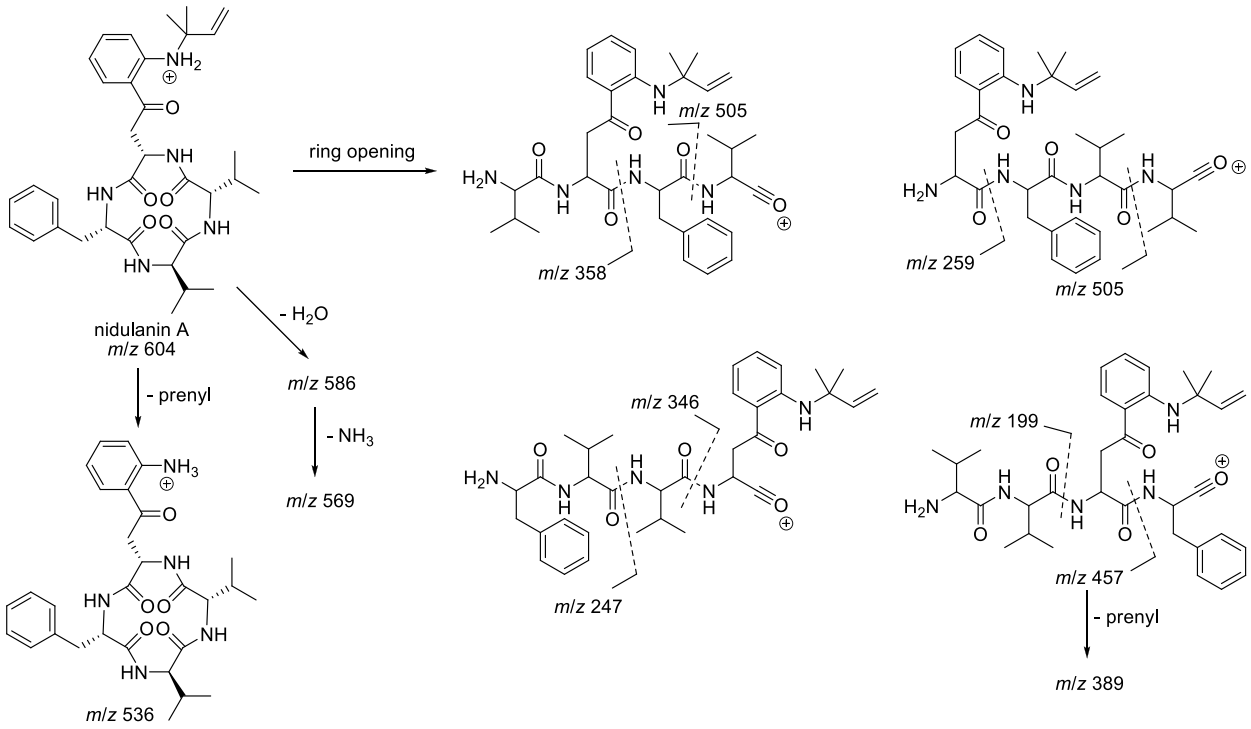

Figure S2. EIC and MS/MS data of nidulanins **5** – **9**. **A.** EIC 536, 620, and 604 trace of extract from LO8111 grown on a GMM plate. **B.** MS/MS spectra of nidulanins (**5** – **9**). **C.** The b-type fragmentations of nidulanin A are illustrated.

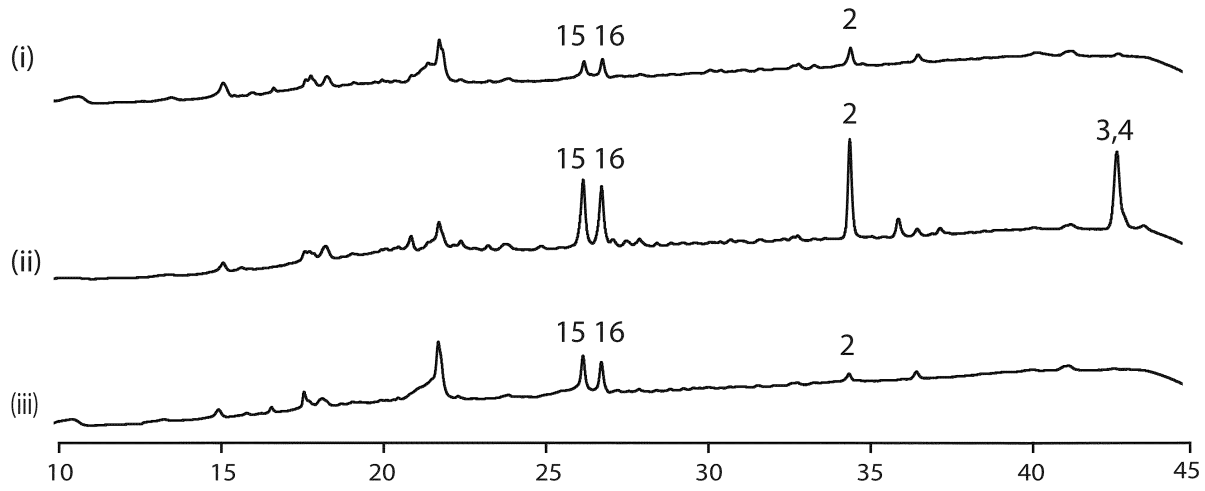

Figure S3. Reinsertion of AN8694 (*mcrA*) returns secondary metabolite production to parental levels. Traces are HPLC UV-Vis total scans (200-600 nm). Growth was on GMM plates and extraction and HPLC conditions were identical to those used for Fig. 5. i. The parental strain LO7543. ii. Strain LO8162 which carries a deletion of AN8694 in LO7543. Iii. Strain 10255 in which AN8694 has been reinserted at the *yA* locus of strain LO8162. All three strains carry a deletion of the sterigmatocystin gene cluster and replacement of AN1242 with *AfriboB*. Sterigmatocystin, nidulanin A and pathway intermediates for these compounds are, thus, not produced. Deletion of AN8694 causes an increase in production of austinol (**15**), dehydroaustinol (**16),** terrequinone (**2**), shamixanthone (**3**) and emericellin (**4**) (the latter two form a single peak under these conditions). Insertion of a functional copy of AN8694 at the *yA* locus returns SM production to levels seen with the parental strain. The peak at 22 min is not yet identified, but it does not correlate with AN8694 presence or absence.

A.

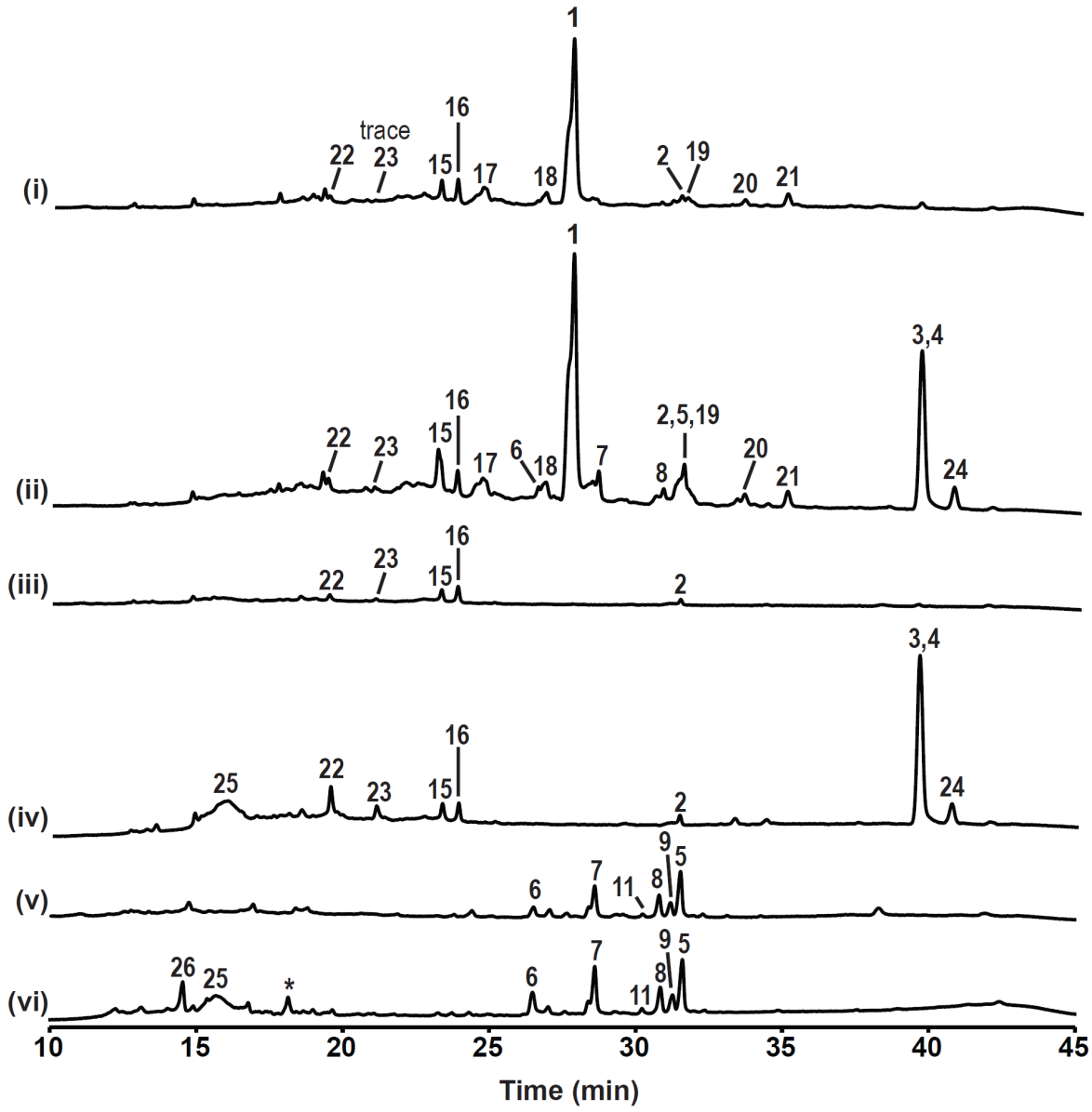

B.

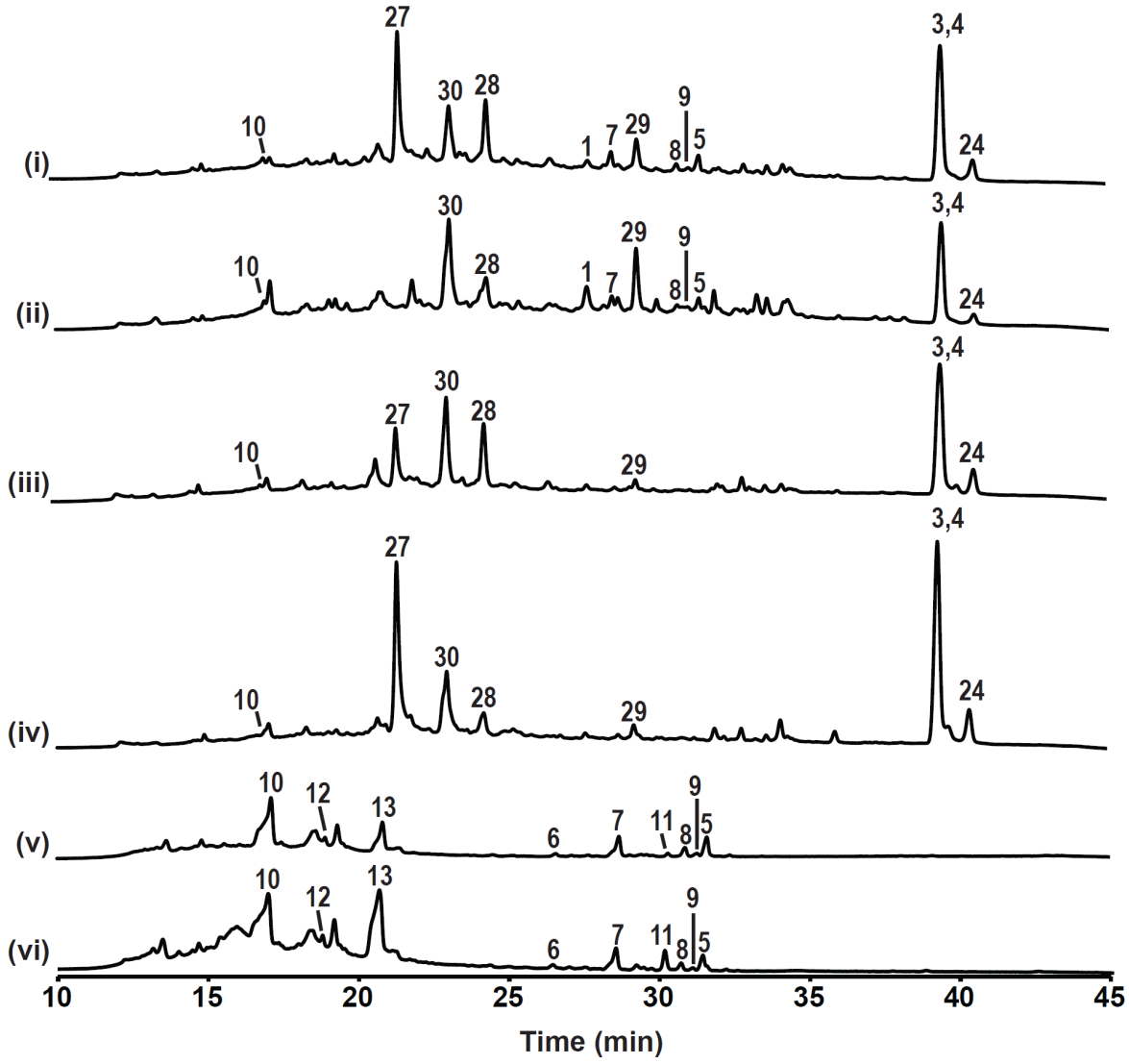

Figure S4. HPLC paired profile scans of parental strains and AN8694 deletion strains. **A.** HPLC UV-Vis total scan (200 – 600 nm) profiles of strains grown on LMM. (i) Parental strain LO1362, (ii) LO8158 a AN8694 deletion strain made from LO1362, (iii) LO7543 parental strain (iv) LO8162 deletion strain made from LO7543, (v) LO8030 parental strain (vi) LO8111 deletion strain made from LO8030. **B.** Same paired parental and deletion strains grown on YAG plates. **1** is sterigmatocystin, **2** is terrequinone, **3** is shamixanthone, **4** is emericellin, **5** is nidulanin A, **6** – **9** are nidulanins (see Figure S1), **10** is cichorine, **11** is aspercryptin, **12** is *N*-(4-carboxybutyl)cichorine, **13** is a *O*-methyl-3-methylorsellinaldehyde dimer, **15** is austinol, **16** is dehydroaustinol, **17** – **21** are sterigmatocystin intermediates, **22** is F9775B, **23** is F9775A, **24** is epishamixanthone, **25** and **26** are unknowns, **27** is asperthecin, **28** is emodic acid, **29** is emodin, **30** is an unknown. Notice that **2**, **5** and **19** co-eluted at 31.6 min; **3** and **4** co-eluted at 39.6 min. *: lumicrome.

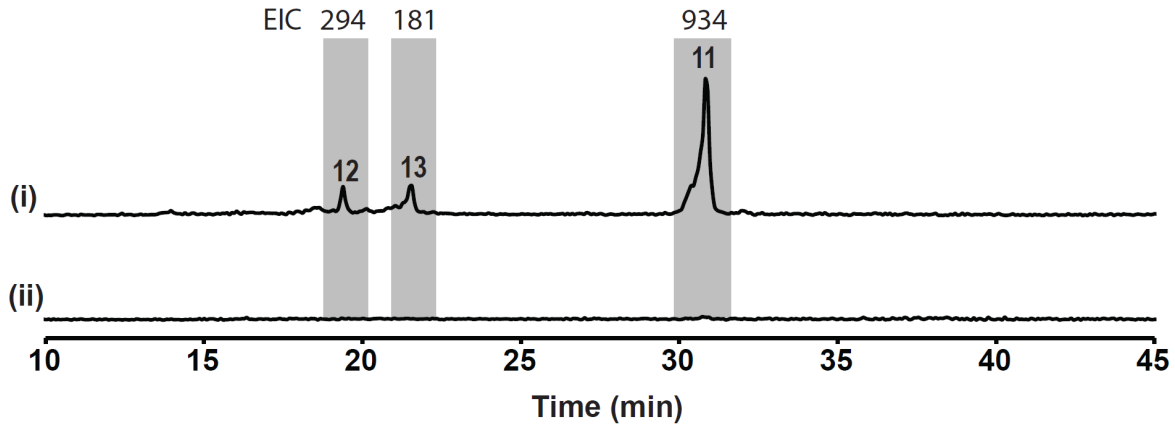

Figure S5. EIC trace at m/z 294, 181, and 934 (positive mode) of extract from (i) parental strain LO8111 and (ii) AN6448Δ LO9345. Strains were grown on YAG plates.

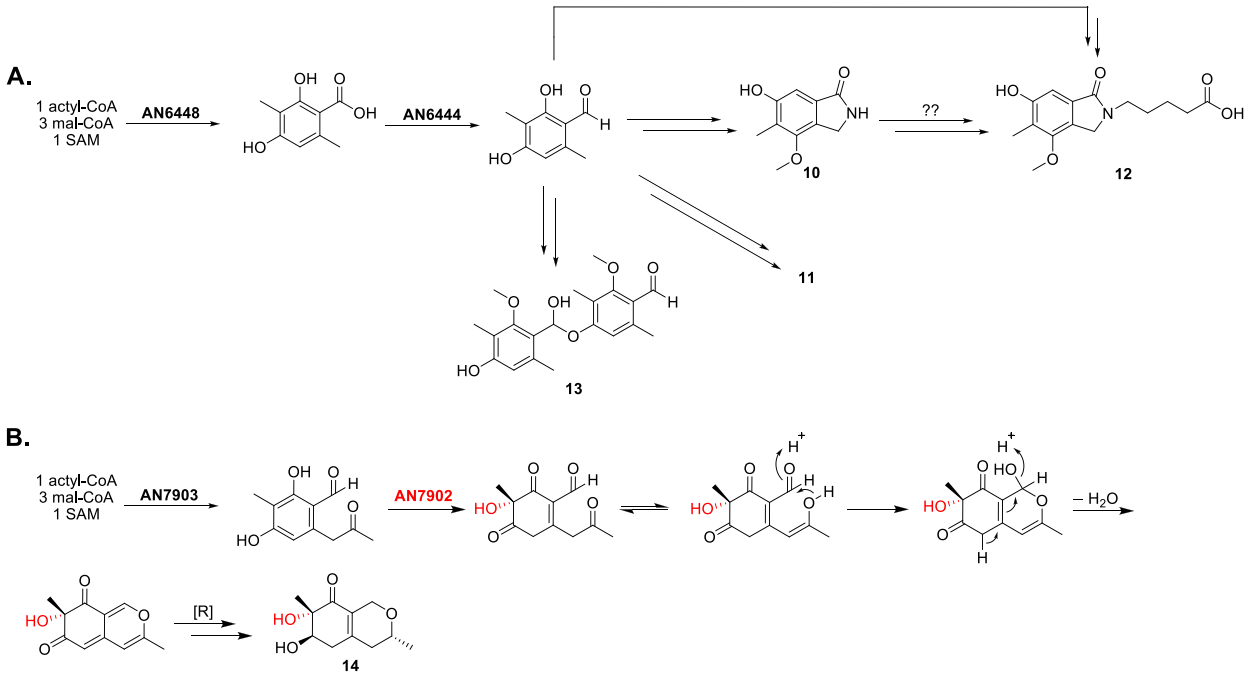

Figure S6. Proposed biosynthesis pathways of **A.** compounds **10** – **13**, and **B.** compound **14**. AN6444 (cicB) is a nonribosomal peptide synthase (NRPS)-like enzyme. A homolog of AN6444, ATEG_03630, has recently been characterized as an aryl-acid reductase (Wang *et al*., 2014). AN7902 has high homology with tropB, a FAD-dependent monooxygenase, which dearomatizes 3-methylorcinaldehyde *via* hydroxylation (Davison *et al*., 2012).

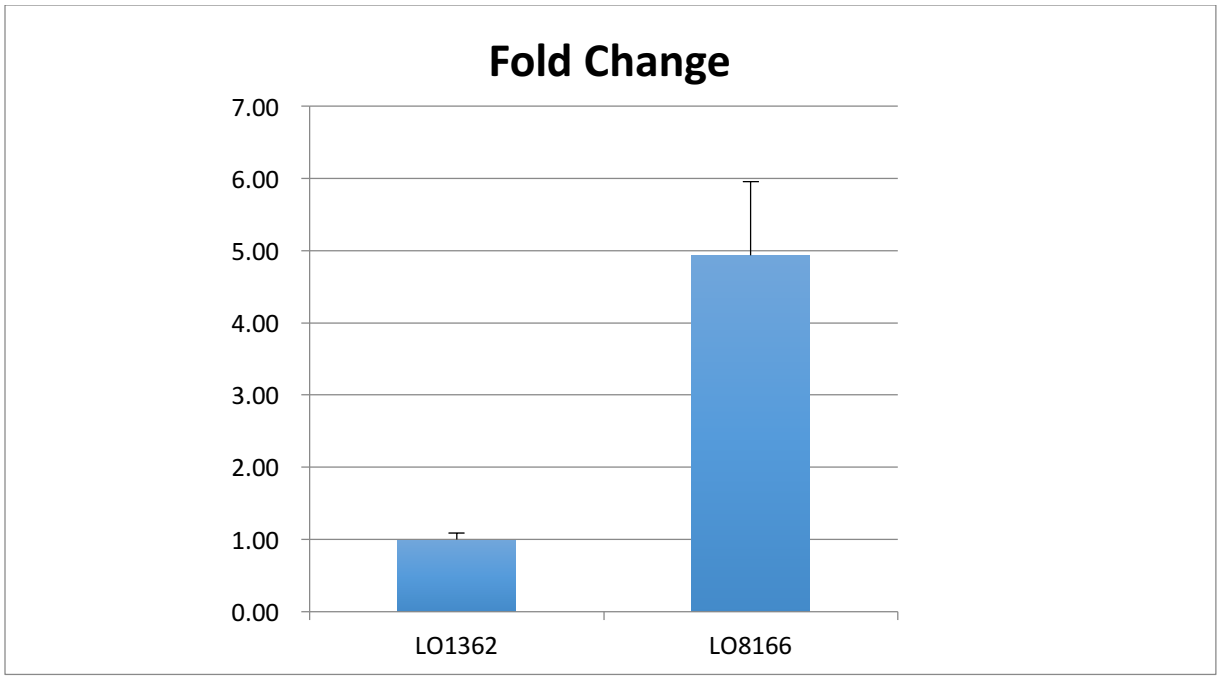

Figure S7. Upregulation of AN8694 (*mcrA*) by the *alcA* promoter. A parental strain, LO1362, and an *alcA*(p)AN8694 strain, LO8166, were grown in liquid lactose minimal medium and *alcA*(p) was induced with 10 mM cyclopentanone. Cultures were harvested 48 h after induction, RNA was purified and quantified by quantitative RTPCR. AN8694 mRNA levels were normalized to actin mRNA levels in both strains. Results are means ± standard error for three experiments.

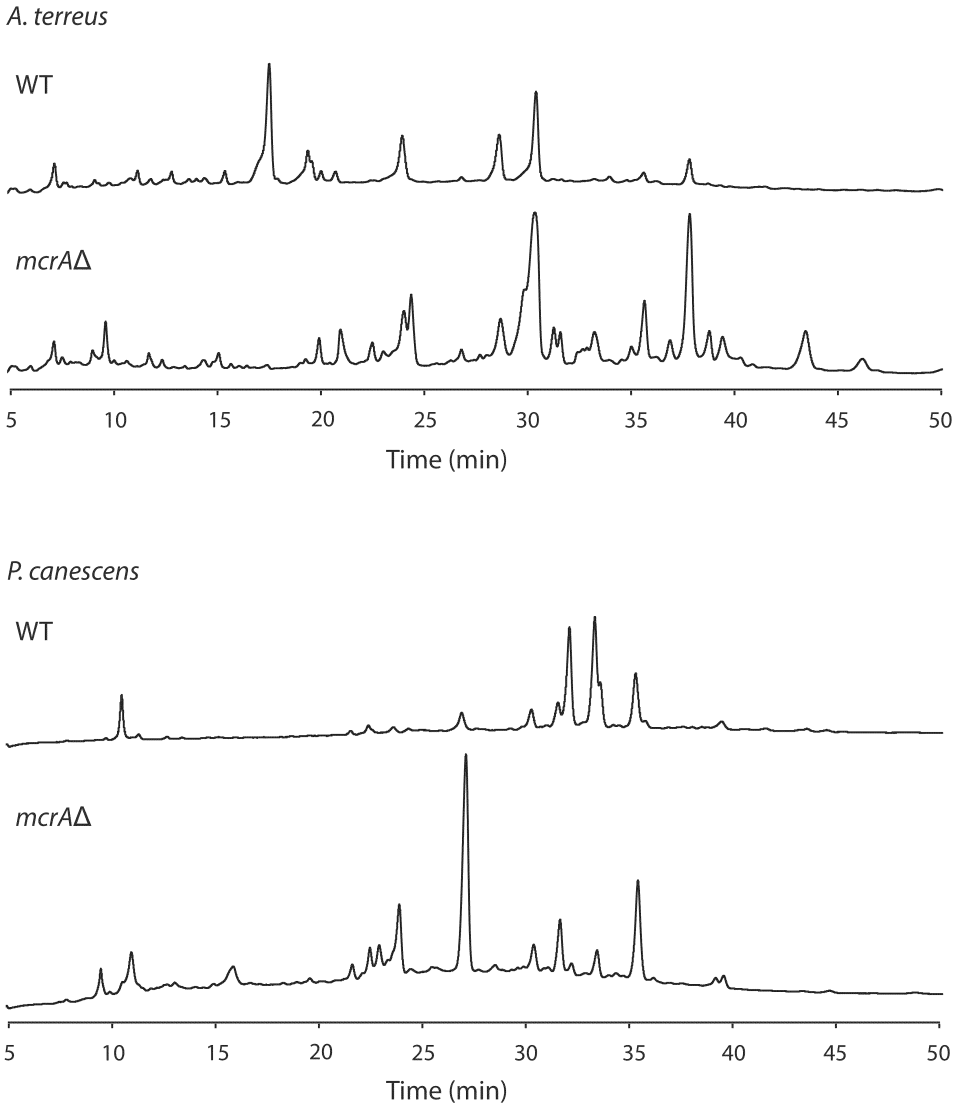

Figure S8. Deletion of *mcrA* homologs alters secondary metabolite production in *A. terreus* and *P. canescens.* These are paired scans of an *A. terreus* parental strain and the same strain with the *A. terreus mcrA* homolog (ATET_07219.1) deleted and a *P. canescens* parental strain and the same strain with the *P. canescens mcrA* homolog (CE25191_2989) deleted. In each case, deletion of the *mcrA* homolog alters the secondary metabolite profile, causing the disappearance of a small number of peaks and the appearance or enhancement of several peaks. Deletion of *mcrA* homologs, thus, stimulates production of compounds not detected in wild-type strains and potentiates discovery of additional secondary metabolites. All traces are UV-Vis scans 200-600 nm.

A. terreus strains were cultivated at 37 °C in LCMM liquid medium (6 g/l NaNO3, 0.52 g/l KCl, 0.52 g/l MgSO4.7H2O, 1.52 g/l KH2PO4, 10 g/l D-glucose, 20 g/l lactose, supplemented with 1 ml/l of Hutner's trace element solution [Hutner *et. al.*, 1950]) at 1×10^6 spore/ml with shaking at 180 rpm. After 18 h of

incubation, the temperature was switched to 30 °C and the culture medium was collected after 72 h. The medium was filtered and extracted with an equal volume of ethyl acetate (EtOAc).

Penicillium canescens strains were cultivated at 26 °C on 10 cm diameter potato dextrose agar plates inoculated at 1×10^7 spores per plate. After 6 days, agar was chopped into small pieces and extracted with 80 ml 1:1 CH_2Cl_2/MeOH. The extract was evaporated *in vacuo* to yield a water residue, which was suspended in 25 ml H_2O and partitioned with EtOAc.

The EtOAc extracts were evaporated *in vacuo*, and dissolved in 1 ml of 20% DMSO in MeOH and a portion (10 µl) was analyzed by high performance liquid chromatography–photodiode array detection–mass spectrometry (HPLC–DAD–MS). The conditions for LC-MS analysis were as previously described (Guo et al., 2013).

The molecular genetic manipulations in *A. terreus* and *P. canescens,* including protoplasting and gene targeting, were carried out as previously described (Guo et al., 2014; Yaegashi et al., 2015). The diagnostic PCR verification strategy is described in Figure S9.

Strains used for Fig. S8

Fungal strain	*mcrA* homolog deleted	Genotype
Aspergillus terreus NIH2624	-	wildtype
CW9002.1, CW9002.2, CW9002.3	ATET_07219.1Δ	*nkuA:: hph*; *pyrG-*, ATEG_06270.1*:: AfpyrG*
Penicillium canescens ATCC10419	-	wildtype
CW9003.1, CW9003.2, CW9003.3	CE25191_2989Δ	*ku70::hph; pyrG-,* CE25191_2989*::PcanpyrG*

Table S1. Primers used to create deletions of *A. terreus* and *P. canescens mcrA* homologs

ATET_07219.1P1	CAG AAT TTG GAG AGC AAA GG
ATET_07219.1P2	CCG AGG CTC TTT CTT TTC TC
ATET_07219.1P3	CGA AGA GGG TGA AGA GCA TTG GAT TGC TGG ACA TTG GGT AG
ATET_07219.1P4	CAT CAG TGC CTC CTC TCA GAC AGT TGT GCA TAC GCT ACA GAC C
ATET_07219.1P5	GTC CGA GAA AGA AGC ACA TC
ATET_07219.1P6	AAG GCG CAA TAC CAT AAC C
CE25191_2989P1	AGA CCT CGG GAT TGG CGA
CE25191_2989P2	GAT TGG CGA CGG TCC ACT
CE25191_2989P3	CGA AGA GGG TGA AGA GCA TTG CGC GTA TTG AGG CGG GTA
CE25191_2989P4	CAG TGC CTC CTC TCA GAC AGA GTA GAT CGT GTG CTG GCC AC
CE25191_2989P5	CTC CCT CGC AGG ATG CAG
CE25191_2989P6	CCT GAC GAC CAG CCC AAG

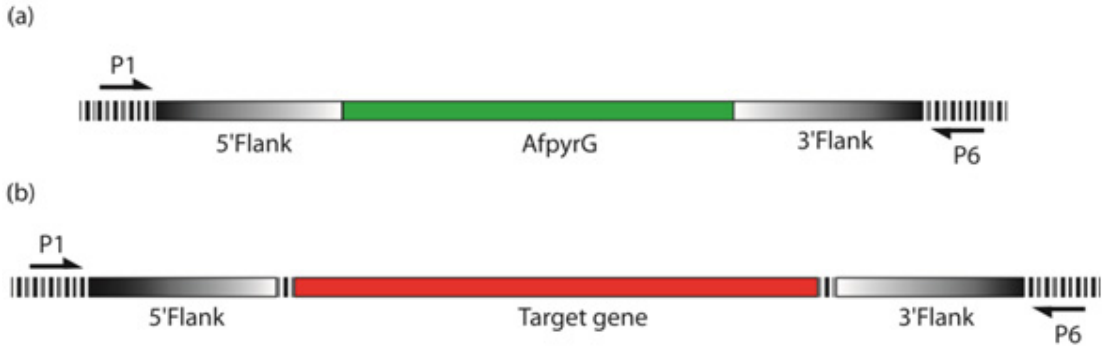

Figure S9. Schematic of the diagnostic PCR strategy for *A. terreus* and *P. canescens*

DNA from transformants was amplified with two primers, P1 from the chromosomal region just outside of the 5' flank of the transforming DNA fragment and P6 from just outside of the 3' flank. Because the target gene is different in size from the *pyrG* gene, which was used as a selectable marker for transformation, the PCR fragment amplified from a correct transformant (a) will be different in size from the fragment amplified if the target gene is intact (b).

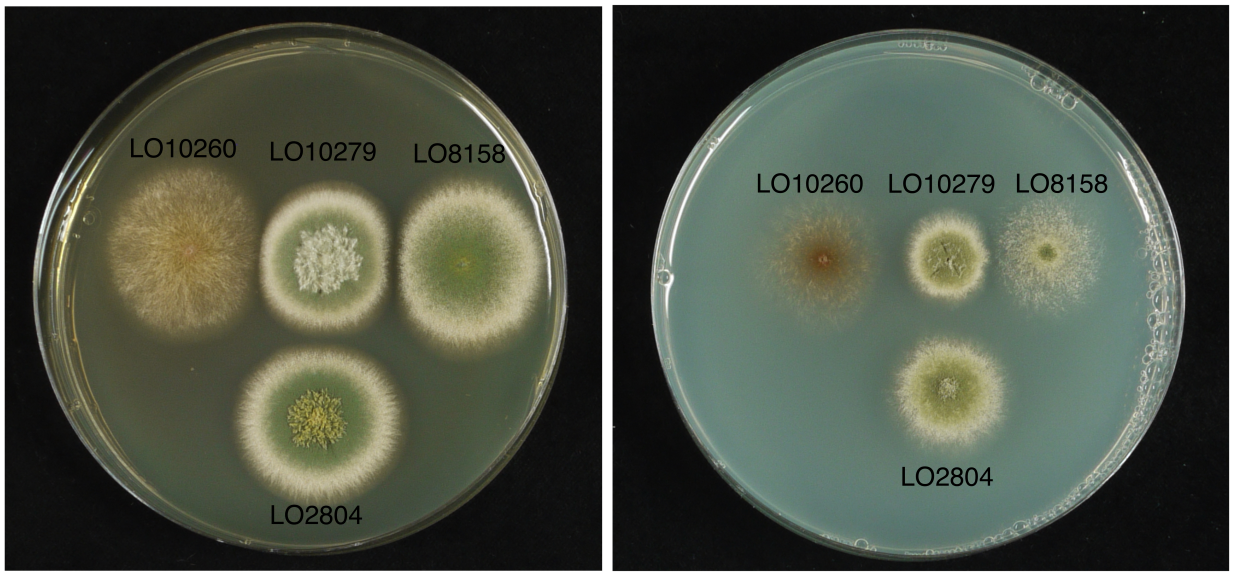

Fig. S10. Deletion of *laeA* affects the growth of *mcrA*Δ. LO8158 (*laeA*$^{+}$, *mcrA*Δ) grows and conidiates well on YAG complete medium (left plate). On glucose minimal medium (right) growth is wispy in comparison with the control strain LO2804 (*laeA*$^{+}$, *mcrA*$^{+}$). The *laeA* deletion strain LO10279 grows and conidiates well on both media although radial growth may be slightly reduced relative to the control. In the *laeA*, *mcrA* double deletion strain LO10260 radial growth is similar to the control but growth is wispy and conidiation is greatly reduced even on YAG. Genotypes are given in Table 1 and media were supplemented for all required nutrients.

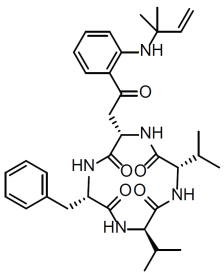

nidulanin A (**5**)

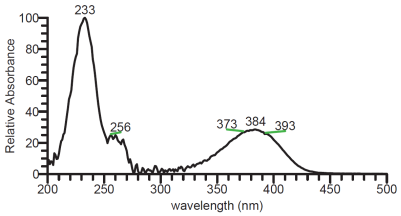

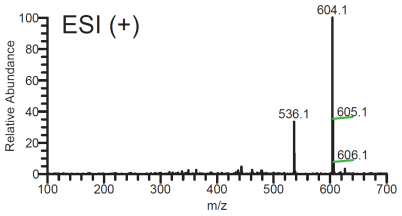

Compound **6**
(nidulanin A - prenyl)

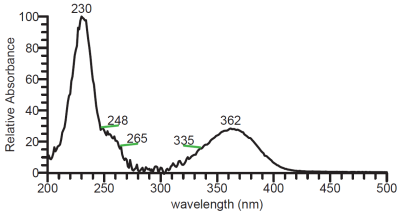

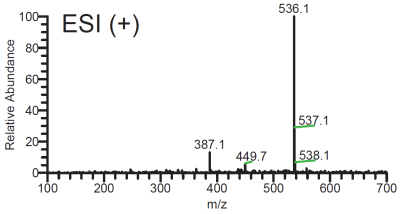

Compound **7**
(nidulanin A + O)

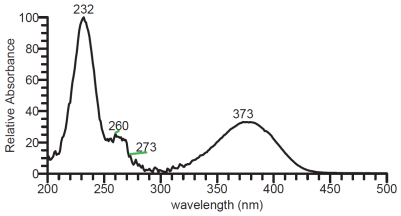

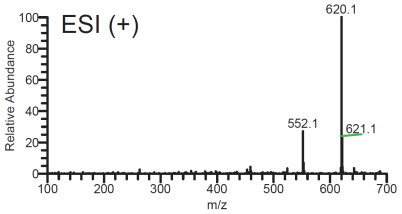

Compound **8**
(nidulanin A analog)

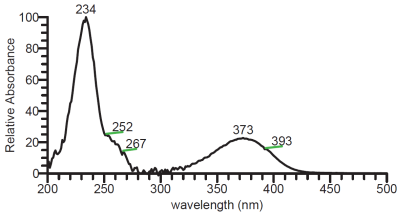

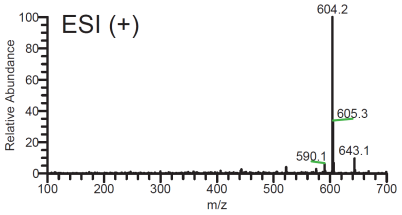

Compound **9**
(nidulanin A analog)

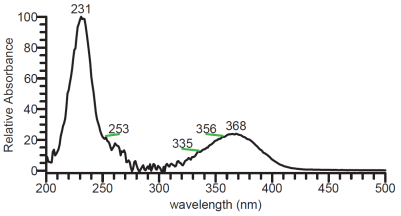

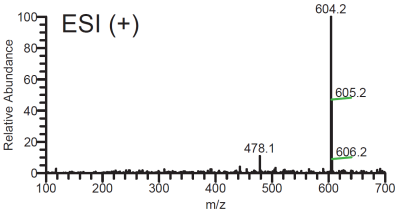

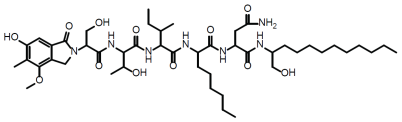

aspercryptin (**11**)

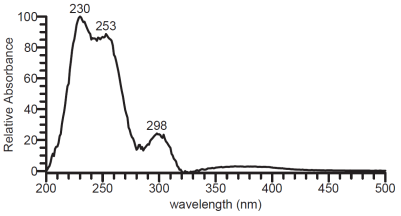

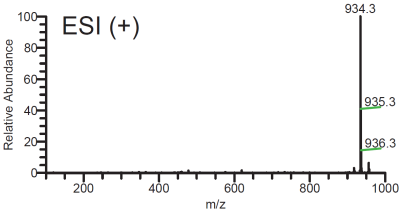

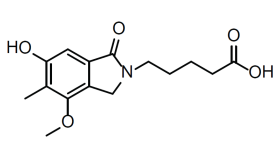

Compound **12**

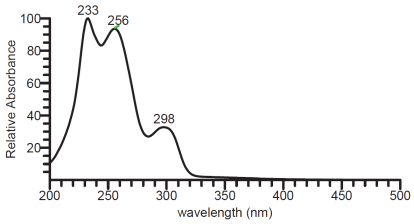

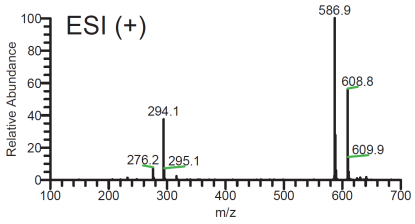

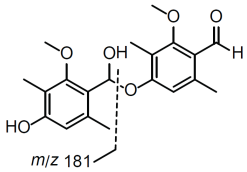

Compound **13**

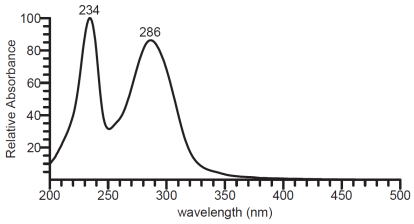

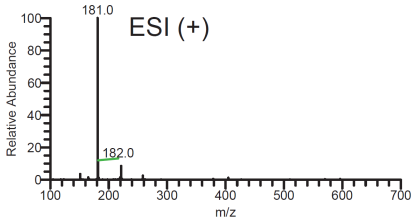

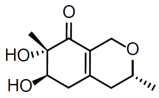

felinone A (**14**)

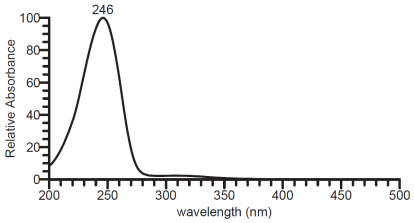

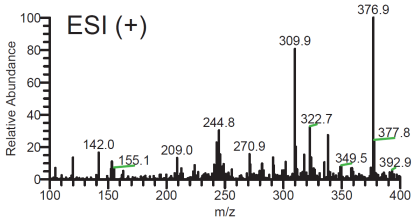

Unknown **17**
(sterigmatocystin intermediate)

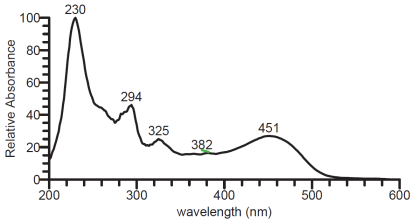

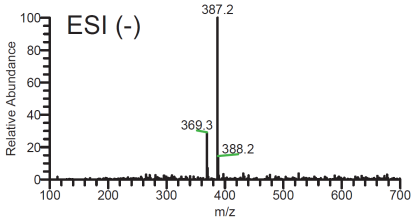

Unknown **18**
(sterigmatocystin intermediate)

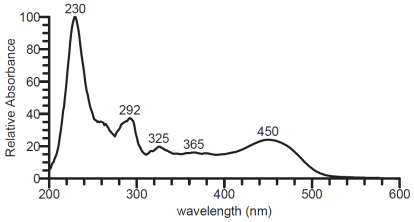

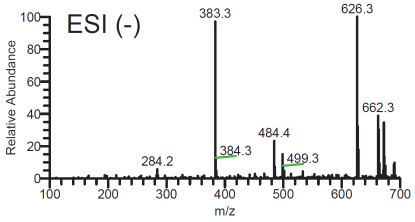

Unknown **19**
(sterigmatocystin intermediate)

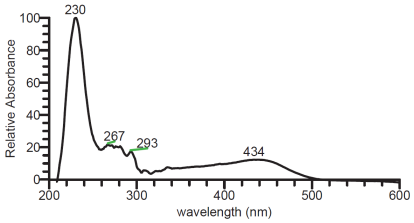

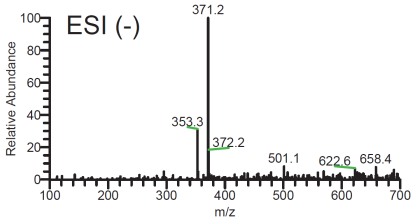

Unknown **20**
(sterigmatocystin intermediate)

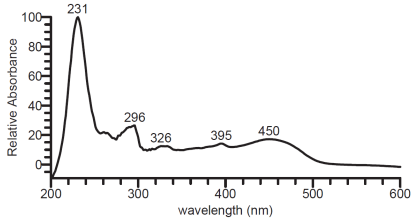

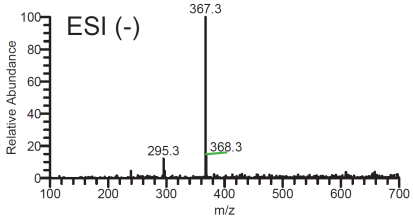

Unknown **21**
(sterigmatocystin intermediate)

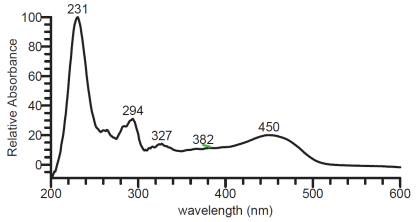

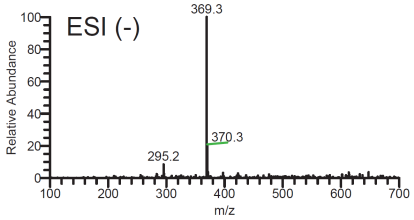

Unknown **25**

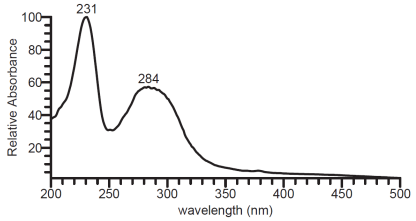

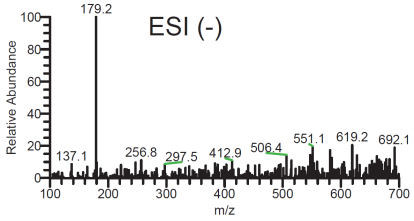

Unknown **26**

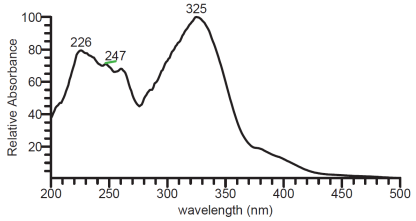

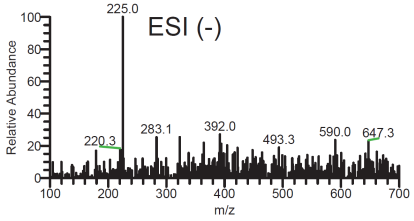

Unknown **30**

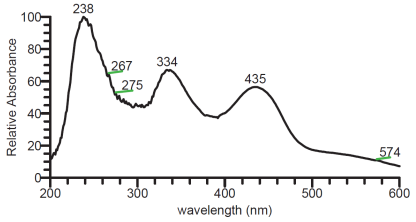

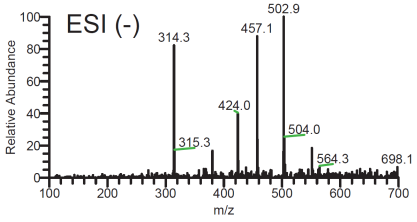

Unknown **31**

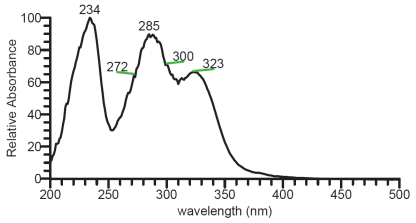

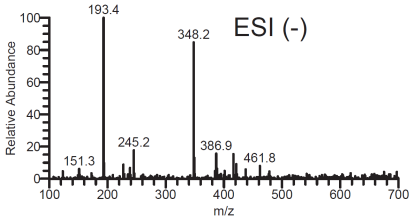

Unknown **32**

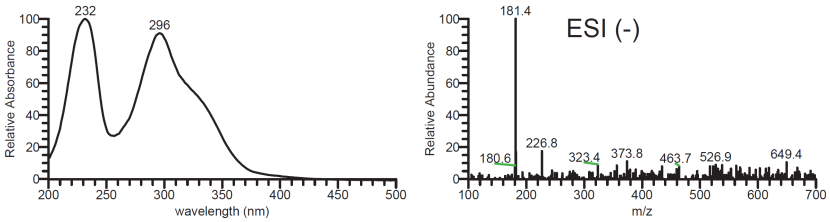

Unknown **33**

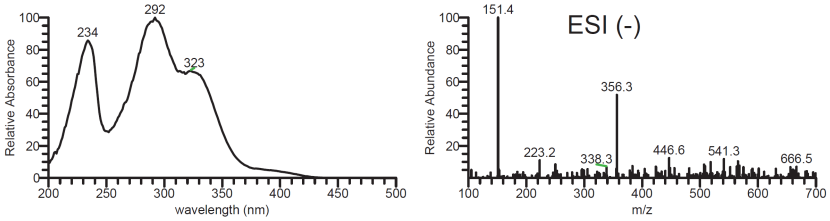

Unknown **36**
(sterigmatocystin intermediate)

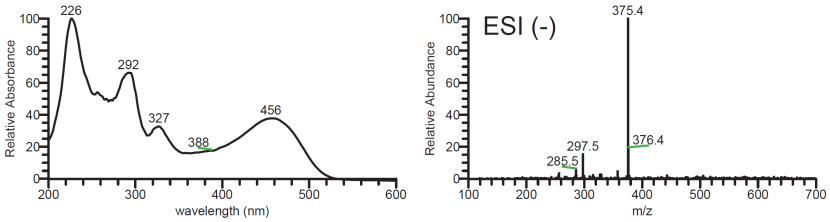

Unknown **37**
(sterigmatocystin intermediate)

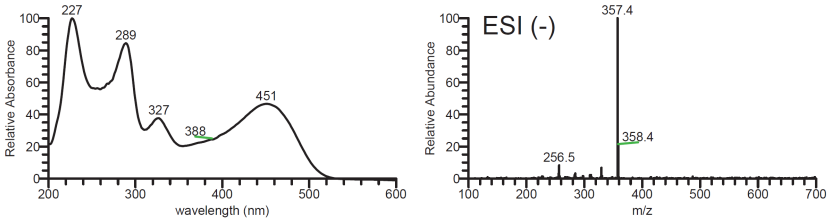

Unknown **38**
(sterigmatocystin intermediate)

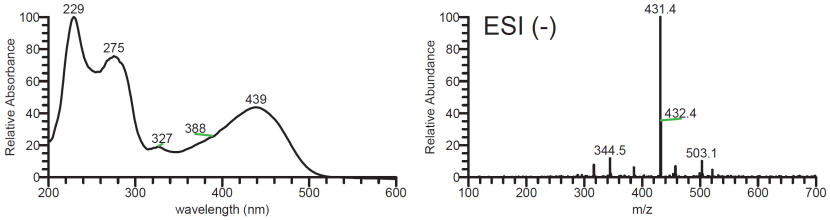

Unknown **39**
(sterigmatocystin intermediate)

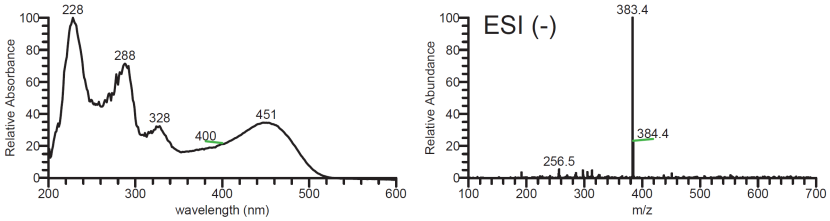

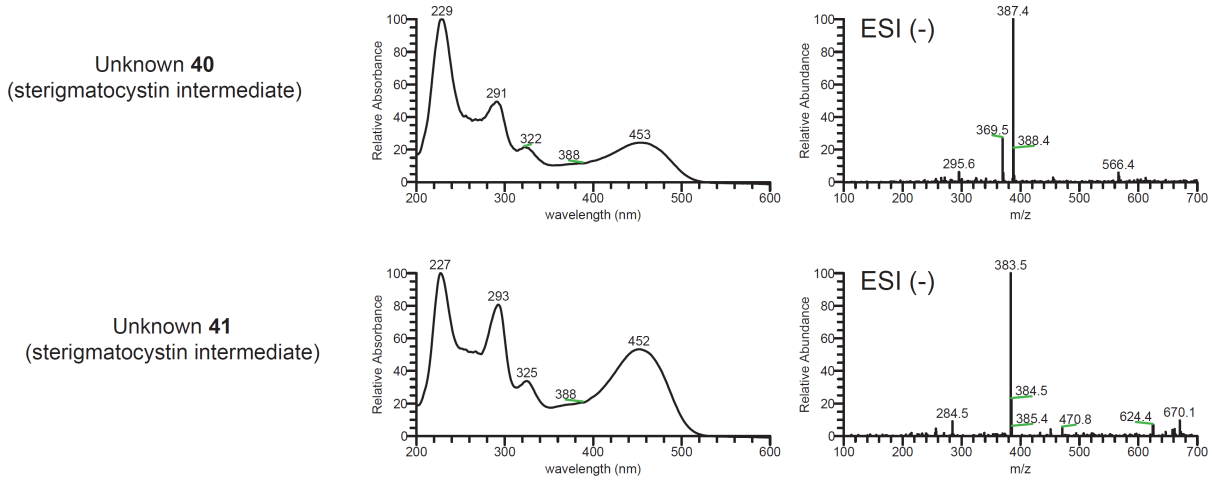

Figure S11. UV-Vis and ESIMS (positive or negative mode) spectra of new and unknown compounds identified in this study. Unknown compounds **17** – **21** and **36** – **39** have similar UV-Vis spectra with averufin, an aflatoxin/sterigmatocystin biosynthesis pathway intermediate (Neilsen and Smedsgaard, 2003). Those compounds were not detected in sterigmatocystin cluster deletion strains, and therefore, were likely to be intermediates or shunt products from the sterigmatocystin biosynthesis pathway. Felinone A (**14**) has very poor ionization in positive or negative mode.

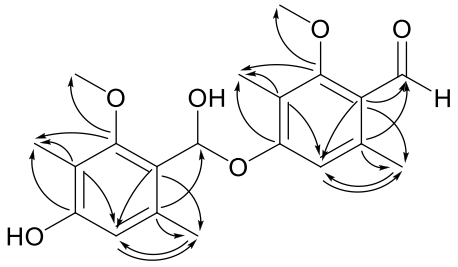

Figure S12. HMBC correlations (C → H) of compound **13**.

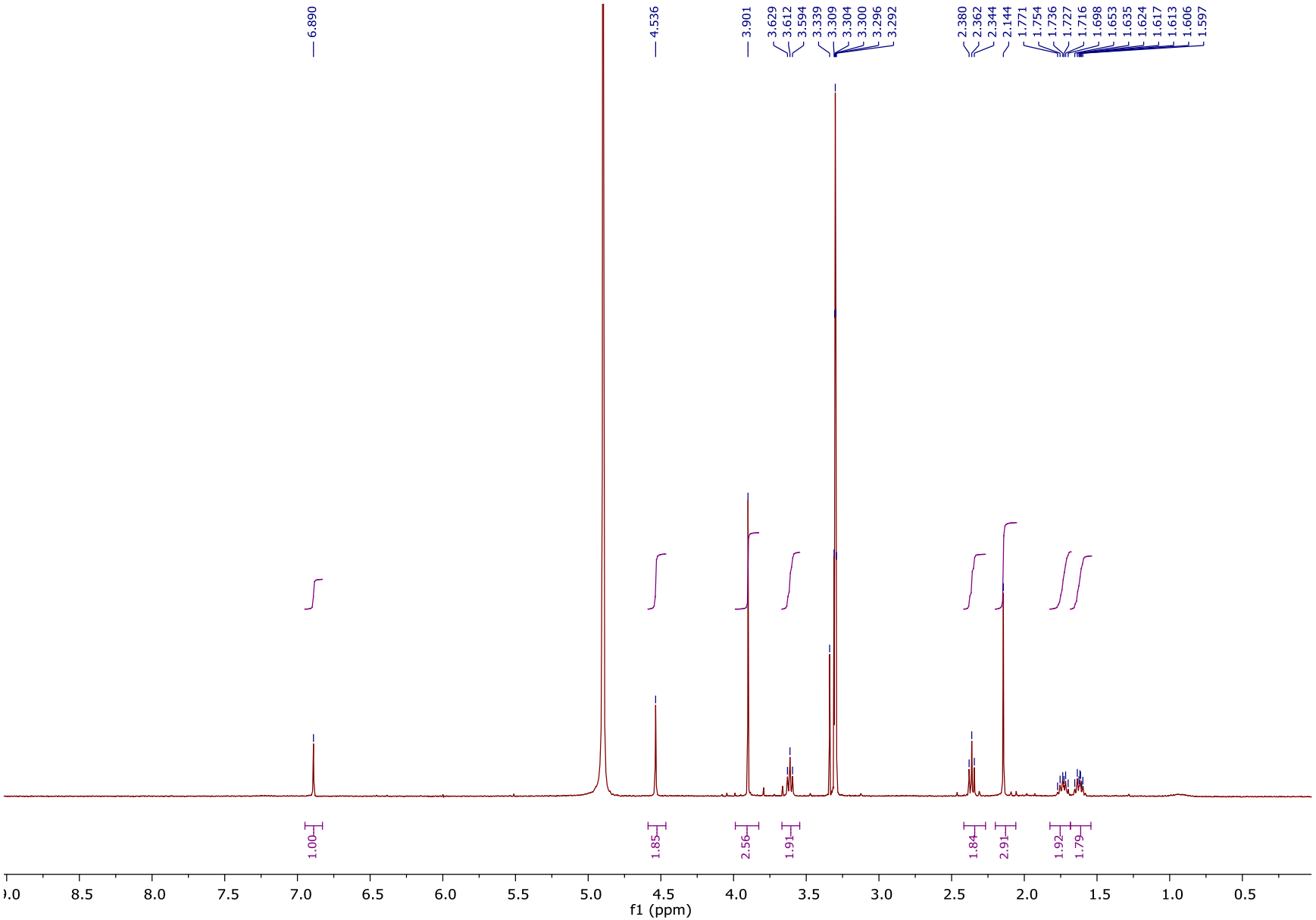

Figure S13. ^{1}H NMR spectrum of *N*-(4-carboxybutyl)cichorine (**12**) in CD_3OD (400 MHz).

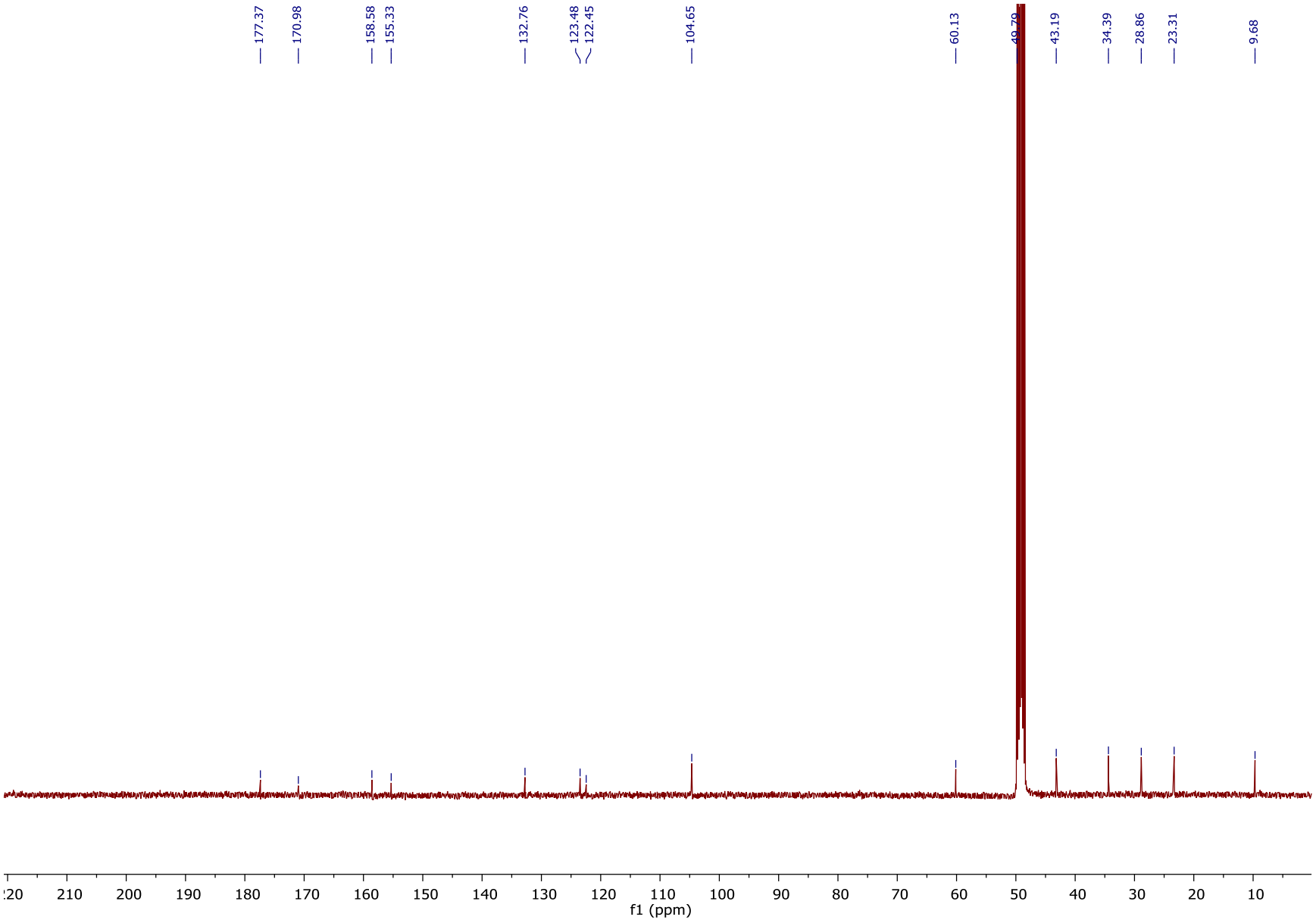

Figure S14. ^{13}C NMR spectrum of *N*-(4-carboxybutyl)cichorine (**12**) in CD_3OD (100 MHz).

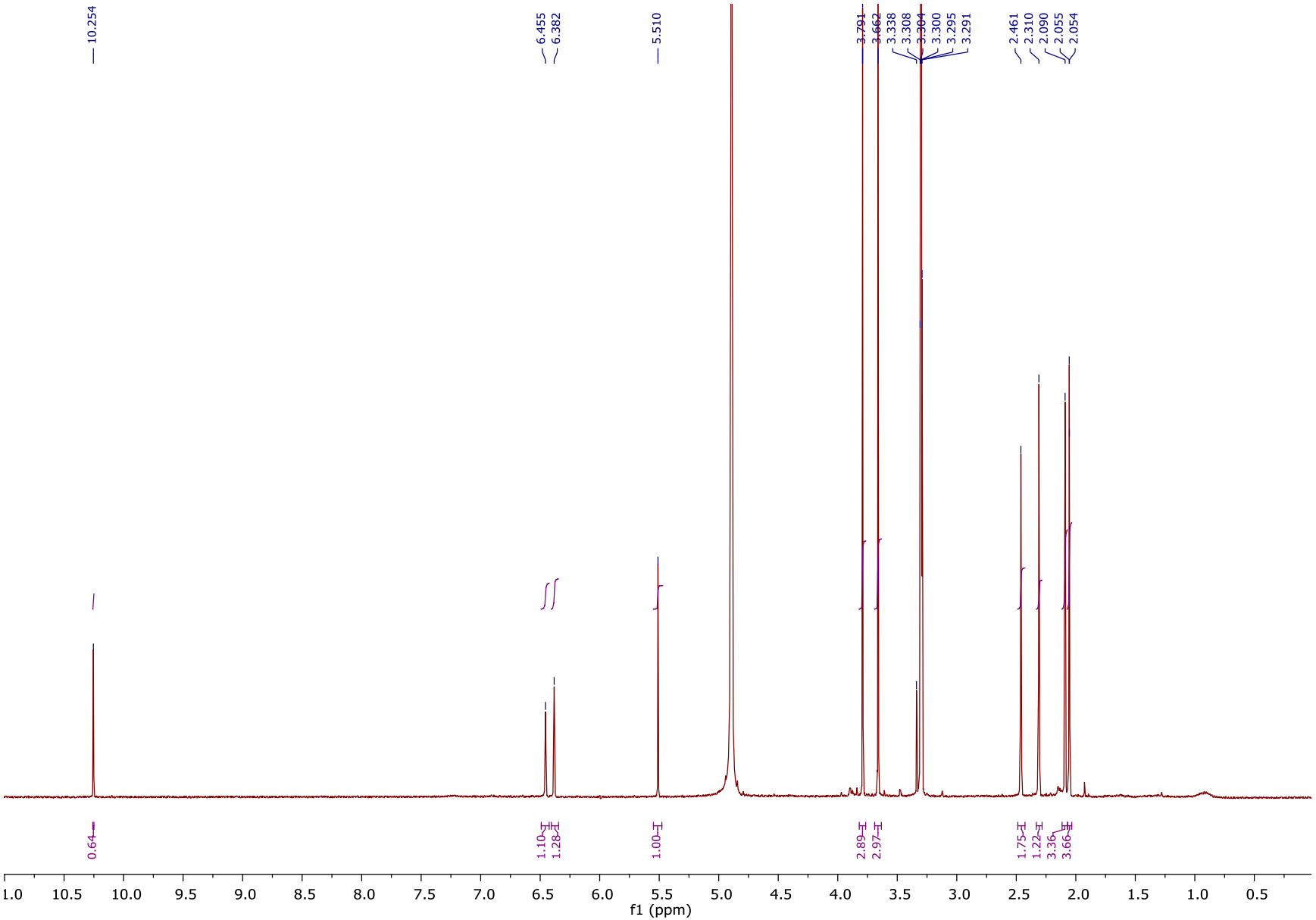

Figure S15. ^{1}H NMR spectrum of *O*-methyl-3-methylorsellinaldehyde dimer (**13**) in CD_3OD (400 MHz).

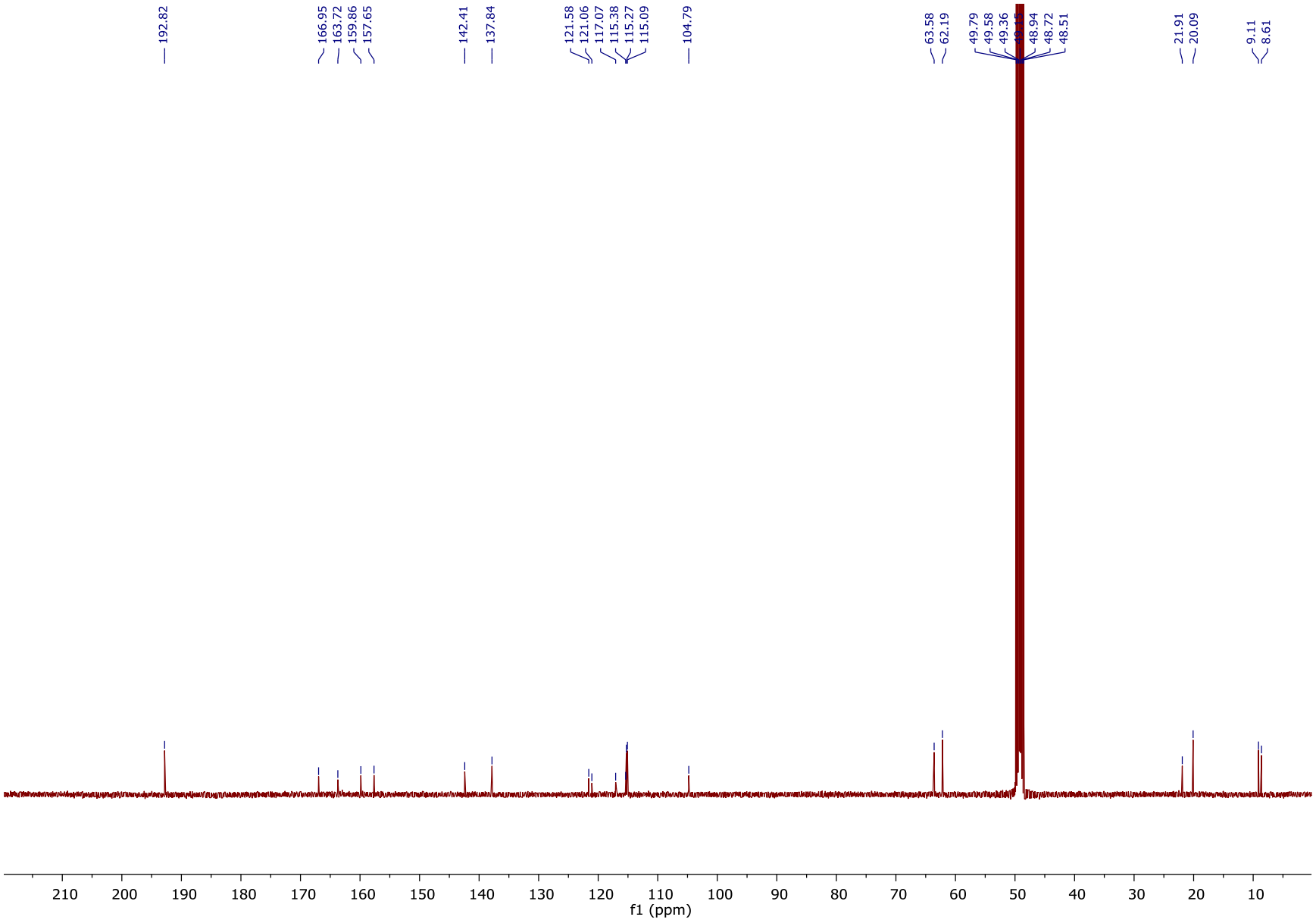

Figure S16. ^{13}C NMR spectrum of *O*-methyl-3-methylorsellinaldehyde dimer (**13**) in CD_3OD (100 MHz).

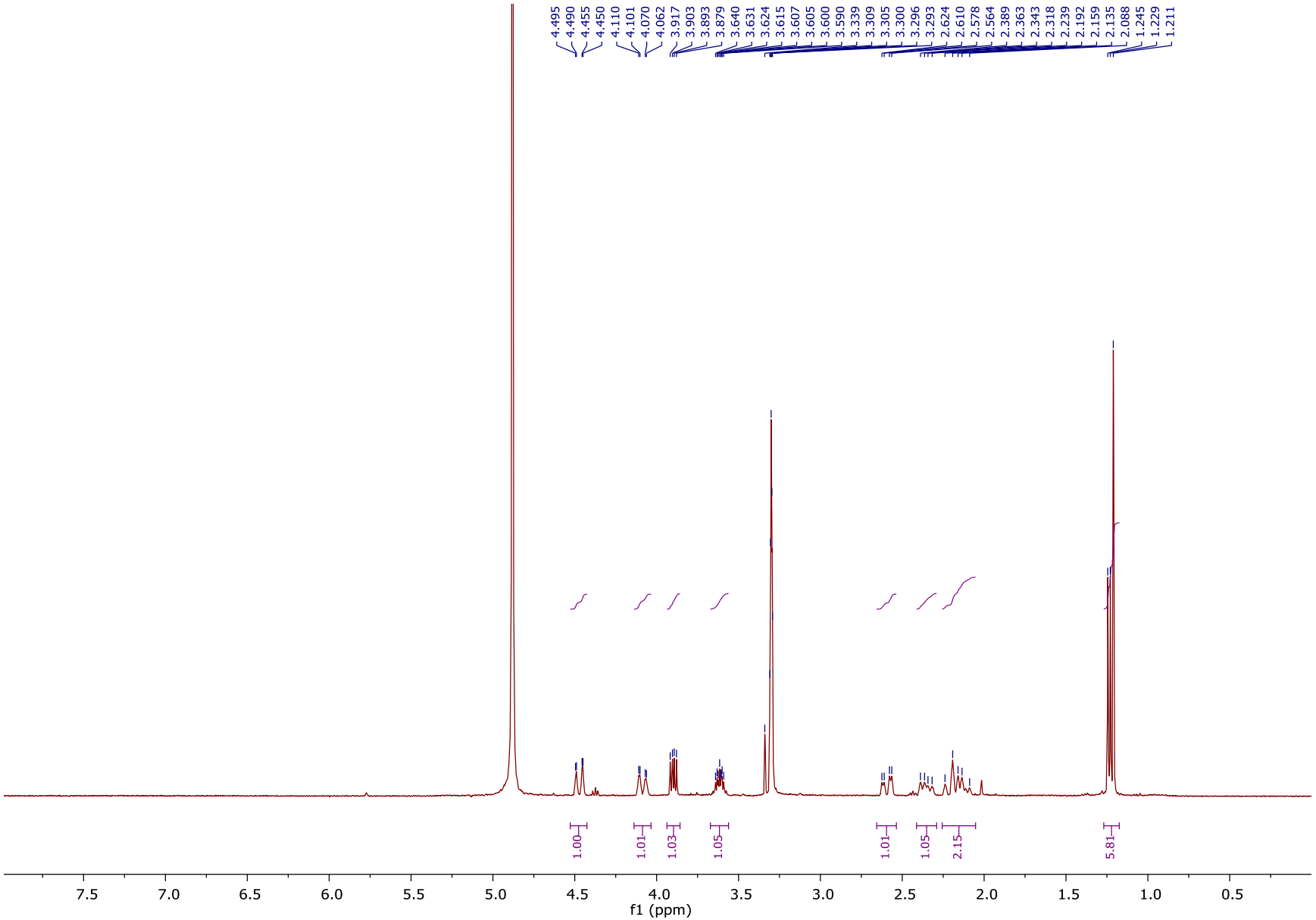

Figure S17. ^{1}H NMR spectrum of felinone A (**14**) in CD_3OD (400 MHz).

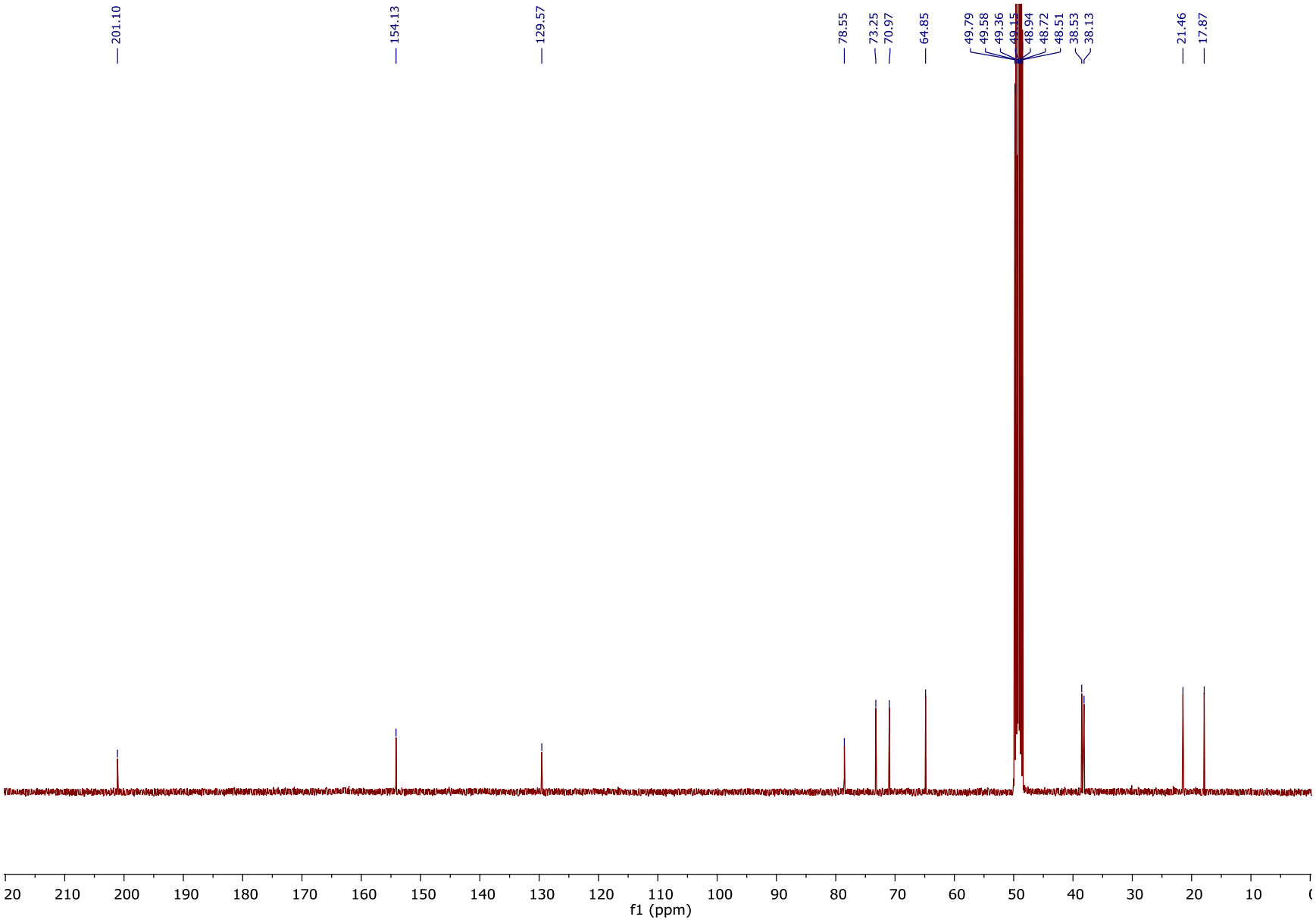

Figure S18. ^{13}C NMR spectrum of felinone A (**14**) in CD_3OD (100 MHz).

Table S2. SMs detected from parental (LO1362, LO7543, LO8030) and AN8694Δ strains (LO8158, LO8162, LO8111) cultured in liquid GMM. Checks indicate the compound was detected.

	LO1362	LO8158	LO7543	LO8162	LO8030	LO8111
sterigmatocystin (**1**)	√	√				
terrequinone (**2**)	√	√	√	√		
shamixanthone (**3**)		√		√		
emericellin (**4**)		√		√		
nidulanin A (**5**)		√				√
nidulanin derivative (**6**)		√				√
nidulanin derivative (**7**)		√				√
nidulanin derivative (**8**)		√				√
nidulanin derivative (**9**)		√				√
cichorine (**10**)						
aspercryptin (**11**)						
N-(4-carboxybutyl)cichorine (**12**)						
compound **13**						
felinone A (**14**)						
austinol (**15**)						
dehydroaustinol (**16**)						
ST intermediate (**17**)						
ST intermediate (**18**)						
ST intermediate (**19**)						
ST intermediate (**20**)						
ST intermediate (**21**)						
F9775B (**22**)		√[a]		√		
F9775A (**23**)		√[a]		√		
epishamixanthone (**24**)						
unknown (**25**)						
unknown (**26**)						
asperthecin (**27**)						
emodic acid (**28**)						
emodin (**29**)						
unknown (**30**)						
emericellamides	√	√	√	√		

[a]The data from three independent cultures were summarized. All secondary metabolites detected were consistent in three independent cultures except for F9775A and B from strain LO8158 which were detected only twice in three independent cultures.

Table S3. SMs detected from a parental strain (LO1362) and *gpdA*(p)AN8694 strains (LO8936, LO8937) cultured under various conditions. Checks indicate that the compound was detected.

	GMM liquid			LMM liquid			YAG plate			GMM plate			LMM plate		
	LO1362	LO8936	LO8937	LO1362	LO8936	LO8937	LO1362	LO8936	LO8937	LO1362	LO8936	LO8937	LO1362	LO8936	LO8937
sterigmatocystin (**1**)	√	√	√	√	√ (↓)[a]	√ (↓)[a]	√	√	√	√	√ (↓)[a]	√ (↓)[a]	√	√ (↓)[a]	√ (↓)[a]
terrequinone (**2**)	√	√	√	√						√[b]			√	√ (↓)[a]	√ (↓)[a]
shamixanthone (**3**)							√								
emericellin (**4**)							√								
nidulanin A (**5**)							√								
nidulanin derivative (**6**)							√								
nidulanin derivative (**7**)							√								
nidulanin derivative (**8**)							√								
nidulanin derivative (**9**)							√								
cichorine (**10**)							√								
aspercryptin (**11**)															
N-(4-carboxybutyl)cichorine (**12**)															
Compound **13**															
felinone A (**14**)															
austinol (**15**)													√		
dehydroaustinol (**16**)													√		
ST intermediate (**17**)													√	√ (↓)[a]	√ (↓)[a]
ST intermediate (**18**)													√	√ (↓)[a]	√ (↓)[a]
ST intermediate (**19**)													√	√ (↓)[a]	√ (↓)[a]
ST intermediate (**20**)													√	√ (↓)[a]	√ (↓)[a]
ST intermediate (**21**)													√	√ (↓)[a]	√ (↓)[a]
F9775B (**22**)		√	√										√[b]	√[b]	√[b]
F9775A (**23**)		√	√										√[b]	√[b]	√[b]
epishamixanthone (**24**)							√								
unknown (**25**)															
unknown (**26**)															
asperthecin (**27**)															
emodic acid (**28**)							√								
emodin (**29**)							√								
unknown (**30**)							√								
emericellamides	√			√			√	√	√	√			√		

[a]The production yield was significantly lower than in the parental (LO1362) strain. [b]Produced at a very low level. Only detected in MS detector but not in DAD.

Table S4. Secondary metabolism genes upregulated > 5X in a *mcrA*Δ strain

Gene	Type of core biosynthetic enzyme	Fold increase in *mcrA*Δ	Mean normalized reads in *mcrA*Δ	Coordinately regulated genes	Product of BGC	Reference
AN1242	NRPS	510	2850	AN11934, AN11080, AN8483	nidulanin A	Andersen *et al.*, 2013
AN2924	NRPS-like	152	393	--	uncharacterized	
AN3230	NR-PKS	17	225	AN3225-3229	aspernidine	Scherlach *et al.*, 2010; Yaegashi *et al.*, 2013
AN2545 AN2547	NRPS HR-PKS	48 61	428 1626	AN2548, AN2549	emericellamide	Chiang *et al.*, 2008
AN10297	NRPS-like	307	61	--	uncharacterized	
AN9005	HR-PKS	18	89	AN9006	uncharacterized	
AN8910	HR-PKS	∞	15	--	uncharacterized	
AN7884	NRPS	9.4	348	AN7873, AN7875-AN7883	aspercryptin	Chiang *et al.*, 2015
AN9314	Entkaurene synthase	∞	13	--	uncharacterized	
AN6431	HR-PKS	∞	10	--	uncharacterized	
AN0150	NR-PKS	6.4	43	--	monodicty-phenone	Bok *et al.*, 2009; Chiang *et al.*, 2010
AN7909	NR-PKS	12	9.6	AN7912	F9775 A, B	Bok *et al.*, 2009; Sanchez *et al.*, 2010.
AN7084	PKS-Like	7.1	20	AN10887	uncharacterized	

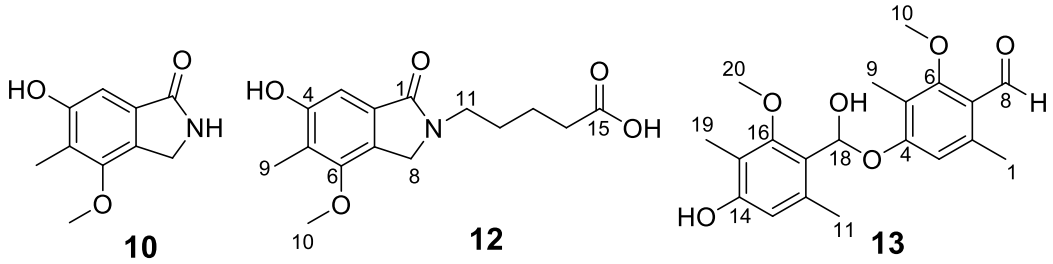

Table S5. NMR spectroscopic data (400 MHz, CD_3OD) for compounds **10**, **12** and **13**.

	Compound **10**		Compound **12**		Compound **13**	
position	δ_C, type	δ_H (*J* in Hz)	δ_C, type	δ_H (*J* in Hz)	δ_C, type	δ_H (*J* in Hz)
.	173.9, C	–	171.0, C	–	21.9, CH_3	2.46 (3H, s)
!	132.4, C	–	132.8, C	–	142.4, C	–
3	104.7, CH	6.92 (1H, s)	104.7, CH	6.89 (1H, s)	115.3, CH	6.46 (1H, s)
4	155.5, C	–	158.6, C	–	163.7, C	–
5	122.9, C	–	122.5, C	–	117.1, C	–
6	158.6, C	–	155.3, C	–	167.0, C	–
7	126.1, C	–	123.5, C	–	121.1, C	–
8	45.1, CH_2	4.47 (2H, s)	49.7, CH_2	4.54 (2H, s)	192.8, CH	10.26 (1H, s)
9	9.7, CH_3	2.15 (3H, s)	9.7, CH_3	2.14 (3H, s)	8.6, CH_3	2.09 (3H, s)
10	60.1, CH_3	3.88 (3H, s)	60.1, CH_3	3.90 (3H, s)	63.6, CH_3	3.79 (3H, s)
11			43.2, CH_2	3.61 (2H, t, 6.8)	20.1, CH_3	2.31 (3H, s)
12			28.9, CH_2	1.73 (2H, m)	137.8, C	–
13			23.3, CH_2	1.62 (2H, m)	115.1, CH	6.38 (1H, s)
14			34.4, CH_2	2.36 (2H, t, 7.2)	157.7, C	–
15			177.4, C	–	115.4, C	–
16					159.9, C	–
17					121.6, C	–
18					104.8, CH	5.51 (1H, s)
19					9.1, CH_3	2.06 (3H, s)
20					62.2, CH_3	3.66 (3H, s)

Construction of Fusion PCR products used in transformations and verification of transformants by diagnostic PCR

As selectable markers, we used the *A. fumigatus pyrG* gene, the *A. fumigatus pyroA* gene, the *A. terreus pyrG* gene, and a pyrithiamine-resistant allele of the *Aspergillus oryzae ptrA* gene. We have constructed cassettes with these markers that allow them to be amplified with either primer pyrGF2 or pyrGF3 (Table S6) at the 5' end, and pyrGRev or, in one case, P4475 at the 3' end, to facilitate fusion PCR.

We replaced the *A. nidulans* AN1242 coding sequence by transformation with a fusion PCR product consisting of: (i) approximately 1.0 kb of AN1242 5' UTR, amplified with primers P4231 and P4232 ending immediately before the initiator ATG codon, (ii) the *A. fumigatus riboB* coding sequence, beginning with the initiator ATG codon, and including 122 bp of 3'UTR, amplified with primers P3954 and P3962, (iii) a selectable marker, either the *A. fumigatus pyrG* gene, with 5' and 3' UTR sequences or the *Afpyro* gene, with 5' and 3' UTR sequences, and (iv) approximately 1.0 kb of AN1242 3' UTR, amplified with primers P4233 and P4234. Transformants were verified by diagnostic PCR using primer pairs: P4229/ P4236, P4229/P3962 and pyrGF3/P4236.

*mcrA*Δ:

mcrA was deleted by transformation with a three-piece fusion PCR product consisting of: (i) approximately 1.0 kb of AN8694 5' UTR, amplified with primer P4511 (ATCCAGGACGGAATGCACG) and P4512, (ii) a selectable marker, and (iii) a fragment consisting of approximately 1.0 kb of AN8694 3' UTR, amplified with primers P4513 and P4514. Transformants were verified by diagnostic PCR using primer pairs: P4509/ P4516, P4509/pyrGRev and pyrGF3/P4516.

To re-insert *mcrA* at the *yA* locus:

To re-insert *mcrA* at the *yA* locus, we transformed with a fusion PCR product consisting of: (i) a fragment carrying approximately 1.0 kb of yA 5' UTR amplified with primers P1748 and P1752, (ii) a selectable marker, (iii) an *A. nidulans* fragment carrying the AN8694 coding seqence plus approximate 500 bp of 5' UTR and approximately 400 bp of 3'UTR made with primers P6782 and P6783, and (iv) a fragment carrying approximately 1.0 kb of *yA* 3' UTR amplified with P5549 and P697. Transformants were verified by diagnostic PCR using primer pairs: P5481/ P4322, P5481/P2986 and P2985/P4322.

gpdA(p)*mcrA*:

To express *mcrA* under control of the *A. nidulans gpdA* promoter, we transformed with a fusion PCR product consisting of: (i) approximately 1.0 kb of AN8694 5' UTR amplified with primers P4511 and P4512 (ii) a selectable marker, (iii) the *gpdA* promoter, amplified with primers P4800 and P2273, and (iv) approximately 1.0 kb of the AN8694 coding sequence, beginning with the initiator codon, amplified with

primers P5154 and P4529. Transformants were verified by diagnostic PCR using primer pairs: P4509/P4529, P4509/pyrGRev, and pyrGF2/ P4529.

alcA(p)*mcrA*:

To express *mcrA* under control of the *A. nidulans alcA* promoter, we transformed with a fusion PCR product consisting of: (i) approximately 1.0 kb of AN8694 5' UTR amplified with primers P4511 and P4527, (ii) a selectable marker, amplified with primers pyrGF2 and P4475, (iii) the *alcA* promoter, amplified with primers P1720 and P1726, and (iv) approximately 1.0 kb of the AN8694 coding sequence, beginning with the initiator codon, amplified with primers P4528 and P4529. Transformants were verified by diagnostic PCR using primer pairs: P4509/P4530, P1726/P4530 and P4509/P1720.

*laeA*Δ:

We deleted *laeA* by transformation with a fusion PCR product consisting of: (i) approximately 1.0 kb of AN0807 5' UTR, amplified with primer P6771 and P6794, (ii) a selectable marker, and (iii) a fragment consisting of approximately 1.0 kb of AN0807 3' UTR, amplified with primers P6773 and P6774. Transformants were verified by diagnostic PCR using primer pairs: P6770/P6776, P6770/P6399, and P6398/P6776.

gpdA(p)*laeA*:

To express *laeA* (AN0807) under control of the *A*. *nidulans gpdA* promoter, we transformed with a fusion PCR product consisting of: (i) approximately 1.0 kb of AN0807 5' UTR amplified with primers P6771 and P6794, (ii) a selectable marker, (iii) the *gpdA* promoter, amplified with primers P4800 and P2273, and (iv) approximately 1.0 kb of the AN0807 coding sequence, beginning with the initiator codon, amplified with primers P6778 and P6779. Transformants were verified by diagnostic PCR using primer pairs: P6770/P6781, and P6770/P6399, P6398/P6781, (or P6770/P4963, P4962/P6781 when the Afpyro marker was used), and P4799/P6776.

alcA(p)*laeA*:

To express *laeA* (AN0807) under control of the *A*. *nidulans alcA* promoter, we transformed with a fusion PCR product consisting of: (i) approximately 1.0 kb of AN0807 5' UTR amplified with primers P6771 and P6794, (ii) a selectable marker, (iii) the *alcA* promoter, amplified with primers P4877 and P1720, and (iv) approximately 1.0 kb of the AN0807 coding sequence, beginning with the initiator codon, amplified with primers P6777 and P6779. Transformants were verified by diagnostic PCR using primer pairs: P6770/P6781, P6770/P6399, and P6398/P6781.

AN6448Δ:

We deleted AN6884 (*pkbA* or *cic*F) by transformation with a fusion PCR product consisting of: (i) approximately 1.0 kb of AN6884 5' UTR, amplified with primers P2103 and P2104, (ii) a selectable marker, and (iii) a fragment consisting of approximately 1.0 kb of AN6884 3' UTR, amplified with primers P2105 and P2106. Transformants were verified by diagnostic PCR using primer pairs: P2102/P2107, P2102/P1713, and P1715/P2107

Table S6. Primers used for *Aspergillus nidulans* constructs and verifications. Italicized nucleotides are tails added to allow fusion PCR.

Primer	Sequence	Function
pyrGF2	CAATGCTCTTCACCCTCTTCG	Forward primer for selectable markers
pyrGF3	GAGTTATTCTGTGTCTGACGAAAT	Alternate forward primer for selectable markers
pyrGRev	CTGTCTGAGAGGAGGCACTGATGC	Reverse primer for selectable markers
P697	GTCGCATCTGTCCTCATGC	Reverse primer for 3' UTR of AN6635 (*yA*)
P1713	GTGAAGACCACGAAATCTTC	Reverse primer, inside *AfpyrG*
P1715	GTTACCGTCTCTGCTGATG	Forward primer, inside *AfpyrG*
P1720	TTTGAGGCGAGGTGATAGGAT	Reverse primer for the *A. nidulans alcA* (AN8979) promoter
P1726	AAAGCTGATTGTGATAGTTCCC	Forward primer for the *A. nidulans alcA* (AN8979) promoter
P1748	GATCTCACGGATCTTGAGAC	Forward primer for 5' UTR of AN6635 (*yA*)
P1752	*CGAAGAGGGTGAAGAGCATTG*CAA GGGAGTCTTGTCTGCTC	Reverse primer for 5' UTR of AN6635 (*yA*), with a tail that anneals to pyrGF2
P2102	GCTCACAGTATGATTTGGATC	Forward primer for 5' UTR of AN6448, 5’ to P2103
P2103	GGAAAGCACTTGGAAGCATAC	Forward primer for 5' UTR of AN6448
P2104	*CGAAGAGGGTGAAGAGCATTG*CGG AGCCATGATGAAAGAAC	Reverse primer for 5' UTR of AN6448 with tail that anneals to pyrGF2
P2105	*GCATCAGTGCCTCCTCTCAGACAG*AC CTAGTCATCTCGCTTAGAG	Forward primer for 3' UTR of AN6448 with tail that anneals to pyrGRev
P2273	TGTGATGTCTGCTCAAGCGG	Reverse primer for the *A. nidulans gpdA* (AN8041) promoter
P2985	CTTCAATGCTACCGCTGTTG	Forward primer, inside *A. oryzae* ptrA gene

P2986	CAACAGCGGTAGCATTGAAG	Reverse primer, inside *A. oryzae* ptrA gene
P3954	ATGTCGAATTTACCGTCCCAT	Forward primer for *AfriboB*, beginning with the initiator ATG codon
P3962	*CGAAGAGGGTGAAGAGCATTG* GAACGTTTGCGCTGCAGAAC	Reverse primer for *AfriboB*, ~ 120 nuceotides 3' to the stop codon, with a tail that anneals to pyrGF2
P4229	GCAACACATGAATGCCATCG	Forward primer for 5' UTR of *A. nidulans* AN1242, 5' to P4231
P4231	CGACCTTGCGTTGGCGAC	Forward primer for 5' UTR of *A. nidulans* AN1242
P4232	*ATGGGACGGTAAATTCGACAT* CTTCACGTCAATTAGGTATTAG	Reverse primer for 5' UTR of *A. nidulans* AN1242, beginning immediately 5' to the ATG initiator codon, and with a tail that anneals to P3954 (beginning of *AfriboB*)
P4233	*GCATCAGTGCCTCCTCTCAGACAG* TCGTTGTTCCATTTGTTTGGC	Forward primer for 3' UTR of *A. nidulans* AN1242 with a tail that anneals to pyrGRev
P4234	TGCAGGCTGACTGACGATG	Reverse primer for 3' UTR of *A. nidulans* AN1242
P4236	CAGAGCTATTTGGGGTGGC	Reverse primer for 3' UTR of *A. nidulans* AN1242, 3' to P4234
P4322	AGAACTATCAGCGAAGTAACC	Reverse primer for 3' UTR of AN6635 (*yA*), 3' to P697
P4475	*GGGAACTATCACAATCAGCTTT* CTGTCTGAGAGGAGGCACTGATGC	pyrGRev with a tail that anneals to P1726
P4509	GTTAGTTAGGGACAGACCAC	Forward primer for AN1242 5' UTR, 5' to P4511
P4511	ATCCAGGACGGAATGCACG	Forward primer for AN1242 5' UTR
P4512	*ATTTCGTCAGACACAGAATAACTC* CAGGCGATGCTGCCGAAG	Reverse primer for AN1242 5' UTR, with tail that anneals to pyrGF3
P4513	*GCATCAGTGCCTCCTCTCA* TCAATGCCCAATATGCTCGG	Forward primer for AN1242 3' UTR, with tail that anneals to pyrGRev
P4514	AACAGACAATGCAGGAACAAC	Reverse primer for AN1242 3' UTR
P4516	GGTGCGTAACGGAGGACG	Reverse primer for AN1242 3' UTR, 3' to P4514
P4527	*CGAAGAGGGTGAAGAGCATG* CAGGCGATGCTGCCGAAG	Reverse primer for AN1242 5' UTR, with tail that anneals to pyrGF2
P4528	*TCCTATCACCTCGCCTCAAA* ATGTCGAACAATCCGAACCC	Forward primer for AN8694, beginning with the initiator ATG codon, with a tail that anneals to P1720
P4529	TTGATGACCTACATGATCCTG	Reverse primer for AN8694, approximately 1.0 kb 3' to the start codon.

P4530	CGAGGTCTCTGATCCAAGG	Reverse primer for AN8694, 3' to P4529.
P4799	*GCATCAGTGCCTCCTCTCAGACAG C* GATCGAGACCTAATACAGCC	Forward primer for *gpdA* (AN 8041) promoter, (nucleotides -1241 to -1223) with a tail that anneals to pyrGRev
P4800	*GCATCAGTGCCTCCTCTCAGACAG C* CACCTTCAGTGGACTCGAG	Forward primer for *gpdA* (AN 8041) promoter, (nucleotides -1197 to -1179, note: the last 'C' of the tail is also in the *gpdA* promoter, i.e. nucleotide -1198 is a C) with a tail that anneals to pyrGRev
P4877	*GCATCAGTGCCTCCTCTCAGACAG* AAAGCTGATTGTGATAGTTCCC	Forward primer for *alcA*(p) with a tail that anneals to pyrGRev
P4962	TCAACGCGGAGCAGGTATG	Forward primer, inside *AfpyroA*
P4963	GATCTCCTTGATCATGCTGG	Reverse primer, inside *AfpyroA*
P5154	*CCGCTTGAGCAGACATCACA* ATGTCGAACAATCCGAACCC	Forward primer for AN8694, beginning with the initiator ATG codon, with a tail that anneals to P2273
P5481	CCATCAGGGTCTCAGAGAC	Forward primer for AN6635 (*yA*) 5' UTR
P5549	GTGAGCTCTCATATTCGTACT	Forward primer for AN6635 *(yA*) 3' UTR
P6398	CAGAAGCAGTACCATGGCG	Forward primer, inside *A. terreus AtpyrG*
P6399	CGGCAAGGATGAGCAGGC	Reverse primer, inside A. terreus *AtpyrG*
P6770	CGGGAAGTTTACGAGGAATC	Forward primer for AN0807 (*laeA*) 5' UTR
P6771	AGTCTGGTTCCTGGAAACTG	Forward primer for AN0807 (*laeA*) 5' UTR
P6773	*GCATCAGTGCCTCCTCTCAGACAG* GGAGGAAAACTGCTAGCGC	Forward primer for AN0807 (*laeA*) 3' UTR with a tail that anneals to pyrGRev
P6774	GATATTGAGTCCTTCCGTATG	Reverse primer for AN0807 (*laeA*) 3' UTR
P6776	TTGACGCTGAAGATGAGGAG	Reverse primer for AN0807 (*laeA*) 3' UTR
P6777	*TCCTATCACCTCGCCTCAAA* ATGTTTGAGATGGGCCCGG	Forward primer for AN0807, beginning with the initiator ATG codon, with a tail that anneals to P1720
P6778	*CCGCTTGAGCAGACATCACA* ATGTTTGAGATGGGCCCGG	Forward primer for AN0807, beginning with the initiator ATG codon, with a tail that anneals to P2273
P6779	GATGCCACGGGTTGAGCG	Reverse primer for AN0807 (*laeA*) ~ 1.0 kb 3' to start
P6781	TCGATGCTCTCTGAGACGG	Reverse primer for AN0807 (*laeA*) ~ 1.0 kb 3' to start

P6782	*GCATCAGTGCCTCCTCTCAGACAG* CATAATCAGAATCCTGAAGCC	Forward primer for AN8694, beginning ~ 500 nucleotides 5' to the initiator ATG codon, with a tail that anneals to pyrGRev
P6783	*AGTACGAATATGAGAGCTCAC* GGATTGAACAGATGGGATGG	Reverse primer for AN8694, beginning ~ 500 nucleotides 3' to the istop codon, with a tail that anneals to P5549
P6794	*CGAAGAGGGTGAAGAGCATTG* ATCGACAGCCGAGTGGAAC	Reverse primer for AN0807 (*laeA*) 5' UTR with a tail that anneals to pyrGF2

References for Supplemental Information

Ahuja, M., Chiang, Y.M., Chang, S.L., Praseuth, M.B., Entwistle, R., Sanchez, J.F. *et al.* (2012) Illuminating the diversity of aromatic polyketide synthases in *Aspergillus nidulans*. *J Am Chem Soc* **134**: 8212-8221.

Andersen, M.R., Nielsen, J.B., Klitgaard, A., Petersen, L.M., Zachariasen, M., Hansen, T.J. *et al.* (2013) Accurate prediction of secondary metabolite gene clusters in filamentous fungi. *Proc Natl Acad Sci U S A* **110**: E99-107.

Bok, J.W., Chiang, Y.-M., Szewczyk, E., Reyes-Domingez, Y., Davidson, A.D., Sanchez, J.F. *et al.* (2009) Chromatin-level regulation of biosynthetic gene clusters. *Nat Chem Biol* **5**: 462-464.

Chiang, Y.M., Ahuja, M., Oakley, C.E., Entwistle, R., Asokan, A., Zutz, C. *et al.* (2016) Development of Genetic Dereplication Strains in Aspergillus nidulans Results in the Discovery of Aspercryptin. *Angew Chem Int Ed Engl* **55**: 1662-1665.

Chiang, Y.-M., Szewczyk, E., Davidson, A.D., Entwistle, R., Keller, N.P., Wang, C.C.C., and Oakley, B.R. (2010) Characterization of the *Aspergillus nidulans* monodictyphenone gene cluster. *Appl Environ Microbiol* **76**: 2067-2074.

Chiang, Y.-M., Szewczyk, E., Nayak, T., Davidson, A.D., Sanchez, J.F., Lo, H.C. *et al.* (2008) Molecular genetic mining of the *Aspergillus* secondary metabolome: discovery of the emericellamide biosynthetic pathway. *Chem Biol* **15**: 527-532.

Davison, J., al Fahad, A., Cai, M., Song, Z., Yehia, S.Y., Lazarus, C.M. *et al.* (2012) Genetic, molecular, and biochemical basis of fungal tropolone biosynthesis. *Proc Natl Acad Sci U S A* **109**: 7642-7647.

Du, F.Y., Li, X.M., Zhang, P., Li, C.S., and Wang, B.G. (2014) Cyclodepsipeptides and other O-containing heterocyclic metabolites from Beauveria felina EN-135, a marine-derived entomopathogenic fungus. *Mar Drugs* **12**: 2816-2826.

Guo, C.J., Knox, B.P., Sanchez, J.F., Chiang, Y.M., Bruno, K.S., and Wang, C.C. (2013) Application of an efficient gene targeting system linking secondary metabolites to their biosynthetic genes in Aspergillus terreus. *Org Lett* **15**: 3562-3565.

Guo, C.J., Sun, W.W., Bruno, K.S., and Wang, C.C. (2014) Molecular genetic characterization of terreic acid pathway in Aspergillus terreus. *Org Lett* **16**: 5250-5253.

Hutner, S.H., Provasoli, L., Schatz, A., and Haskins, C.P. (1950) Some approaches to the study of the role of metals in the metabolism of microorganisms. *Proc Am Philos Soc* **94**: 152-170.

Nielsen, K.F., and Smedsgaard, J. (2003) Fungal metabolite screening: database of 474 mycotoxins and fungal metabolites for dereplication by standardised liquid chromatography-UV-mass spectrometry methodology. *J Chromatogr A* **1002**: 111-136.

Sanchez, J.F., Chiang, Y.-M., Szewczyk, E., Davidson, A.D., Ahuja, M., Oakley, C.E. *et al.* (2010) Molecular genetic analysis of the orsellinic acid/F9775 gene cluster of *Aspergillus nidulans*. *Mol Biosyst* **6**: 587-593.

Sanchez, J.F., Entwistle, R., Corcoran, D., Oakley, B.R., and Wang, C.C.C. (2012) Identification and molecular genetic analysis of the cichorine gene cluster in *Aspergillus nidulans*. *Med Chem Commun* **3**: 997-1002.

Scherlach, K., Schuemann, J., Dahse, H.M., and Hertweck, C. (2010) Aspernidine A and B, prenylated isoindolinone alkaloids from the model fungus Aspergillus nidulans. *J Antibiot (Tokyo)* **63**: 375-377.

Wang, M., Beissner, M., and Zhao, H. (2014) Aryl-aldehyde formation in fungal polyketides: discovery and characterization of a distinct biosynthetic mechanism. *Chem Biol* **21**: 257-263.

Yaegashi, J., Praseuth, M.B., Tyan, S.W., Sanchez, J.F., Entwistle, R., Chiang, Y.M. *et al.* (2013) Molecular Genetic Characterization of the Biosynthesis Cluster of a Prenylated Isoindolinone Alkaloid Aspernidine A in Aspergillus nidulans. *Org Lett* **15**: 2862-2865.

Yaegashi, J., Romsdahl, J., Y.-M., C., and Wang, C.C.C. (2015) Genome mining and molecular characterization of the biosynthetic gene cluster of a diterpenic meroterpenoid, 15-deoxyoxalicine B, in *Penicillium canescens*. *Chem Sci* **6**: 6537-6544.